Energy, Mines and Resources Canada
Énergie, Mines et Ressources Canada

CANMET
Canada Centre for Mineral and Energy Technology
Centre canadien de la technologie des minéraux et de l'énergie

SPOC
Simulated Processing of Ore and Coal

Chapter 4.1 Industrial Ball Mill Modelling

Energy, Mines and Resources Canada
Énergie, Mines et Ressources Canada

CANMET

Canada Centre for Mineral and Energy Technology
Centre canadien de la technologie des minéraux et de l'énergie

The SPOC Manual

Chapter 4.1 Industrial Ball Mill Modelling

Industrial Ball Mill Modelling: Documented Application of the Kinetic Model

R. Spring, C. Larsen and A. Mular

Editor: D. Laguitton

Contributor: F. Flament

Mineral Processing Plant Simulation
Minerals Research Program
Mineral Sciences laboratories

SP85-1/4.1E

Available in Canada through

Authorized Book Agents
and other bookstores

or by mail from

Canadian Government Publishing Centre
Supply and Services Canada
Ottawa, Canada K1A 0S9

Catalogue No.: M38-16/4.1-1985E
ISBN 0-660-11863-7

Canada: $7.00
Other Countries: $8.40

Price subject to change without notice
Disponible en français

THE SPOC MANUAL

The **SPOC*** manual consists of eighteen chapters, published separately. Their numbers and short titles are as follows:

1. Summary
2. Sampling Methodology
2.1 SAMBA Computer Program
2.2 Grinding Circuit Sampling
3. Material Balance
3.1 BILMAT Computer Program
3.2 MATBAL Computer Program
4. Modelling and Simulation
4.1 Industrial Ball Mill Modelling
5. Unit Models: Part A
5.1 Unit Models: Part B
5.2 Unit Models: Part C
6. Flowsheet Simulators
7. Model Calibration
7.1 STAMP Computer Program
7.2 FINDBS Computer Program
7.3 RTD and MIXERS Computer Programs
8. Miscellaneous Computer Programs

These chapters are available from: CANMET, Energy, Mines and Resources Canada
Technology Information Division
555 Booth Street
Ottawa, Ontario

*Simulated Processing of Ore and Coal

FOREWORD

High energy costs and depleting ore reserves combine to make process evaluation and optimization a challenging goal in the 80's. The spectacular growth of computer technology in the same period has resulted in widely available computing power that can be distributed to the most remote mineral processing operations. The SPOC project, initiated at CANMET in 1980, has undertaken to provide Canadian industry with a coherent methodology for process evaluation and optimization assisted by computers. The SPOC Manual constitutes the written base of this methodology and covers most aspects of steady-state process evaluation and simulation. It is expected to facilitate industrial initiatives in data collection and model upgrading.

Creating a manual covering multidisciplinary topics and involving contributions from groups in universities, industry and government is a complex endeavour. The reader will undoubtedly notice some heterogeneities resulting from the necessary compromise between ideals and realistic objectives or, more simply, from oversight. Critiques to improve future editions are welcomed.

D. Laguitton
SPOC Project Leader
Canada Centre for Mineral and Energy Technology

AVANT-PROPOS

La croissance des coûts de l'énergie et l'appauvrissement des gisements ont fait de l'évaluation et de l'optimisation des procédés un défi des années 80 au moment même où s'effectuait la dissémination de l'informatique jusqu'aux concentrateurs les plus isolés. Le projet SPOC, a été lancé en 1980 au CANMET, en vue de développer pour l'industrie canadienne, une méthodologie d'application de l'informatique à l'évaluation et à l'optimisation des procédés minéralurgiques. Le Manuel SPOC constitue la documentation écrite de cette méthodologie et en couvre les différents éléments. Les retombées devraient en être une vague nouvelle d'échantillonnages et d'amélioration de modèles.

La rédaction d'un ouvrage couvrant différentes disciplines et rassemblant des contributions de groupes aussi divers que les universités, l'industrie et le gouvernement est une tâche complexe. Le lecteur notera sans aucun doute des ambiguïtés ou contradictions qui ont pu résulter de la diversité des sources, de la traduction ou tout simplement d'erreurs. La critique constructive est encouragée afin de parvenir au format et au contenu de la meilleure qualité possible.

D. Laguitton
Chef du projet SPOC,
Centre canadien de la technologie des minéraux et de l'énergie

ABSTRACT

A simple kinetic ball mill model proved adequate after testing with 100 sets of industrial grinding data. The essential components of the model are (a) a breakage function determined from laboratory tests; (b) a mixers-in-series residence time distribution; and (c) a selection function derived from industrial data. Results show that the absolute selection function (S_iH) is statistically invariant with changes in feedrate, feedsize distribution, and pulp density over the normal operating range. All the experimental and calculational procedures used in the calibration of the model are fully documented. This includes an examination of model residuals and a discussion of model reliability.

RÉSUMÉ

Un modèle cinétique simple de broyeur à boulets s'est avéré suffisant pour simuler 100 régimes stationnaires échantillonnés en usine. Les éléments de base du modèle sont: (a) la fonction de broyage, déterminée par des essais en laboratoire, (b) une distribution de temps de séjour décrite par un modèle de mélangeurs en série, et (c) une fonction de sélection déterminée à partir de mesures obtenues en usine. Les résultats montrent que la fonction de sélection absolue (S_iH) est statistiquement constante quel que soit le débit, la distribution granulométrique ou le pourcentage de solides dans l'alimentation. Les méthodes de mesure et de calcul utilisées pour calibrer le modèle sont exposées en détail, de même qu'une discussion des résidus et de la fiabilité du modèle.

ACKNOWLEDGEMENTS

The SPOC project has benefited from such a wide range of contributions throughout the industry, the university, and the government sectors that a nominal acknowledgement would be bound to make unfair omissions. The main groups that contributed are: the various contractors who completed project elements; the Industrial Steering Committee members who met seven times to provide advice to the project leader; the various users of project documents and software who provided feedback on their experience; the CANMET Mineral Sciences Laboratories staff members who handled the considerable in-house task of software development, maintenance, and documentation; the EMR Computer Science Centre staff who were instrumental in some software development; and the CANMET Publications Section. Inasmuch as in a snow storm, every flake is responsible, their contributions are acknowledged.

CONTENTS

TABLES

FIGURES

1. INTRODUCTION

Many researchers have contributed to the development and refinement of ball mill models (1,2,3,4). Based on their work, it is now possible to present a reasonably complete model which is detailed in a related report (5). Its essential components are reiterated here.

Statement 1 — Grinding is governed by two independent functions: breakage (**b**) and selection (**S**).

The breakage distribution function describes the suite of daughter particles produced by a single breakage event. Specifically, the breakage element $\mathbf{b}_{ij}$ is the weight fraction of particles in size interval i formed by the breakage of a larger particle in size interval j. In this context, *i* or *j* refers to a size fraction with *i=1* being the top size fraction and *i=n* being the pan fraction.

The selection function measures the rate at which breakage events occur for each particle size.

Statement 2 — Grinding is a first-order rate process.

$$\frac{dP_i}{dt} = -S_iP_i \qquad \text{Eq 1}$$

(P_i = weight fraction in size interval ***i***)

Particles in any given size interval break at a rate proportional only to the weight of particles *in that interval*. The proportionality constant is independent of time and independent of other sized particles.

Statements 1 and 2 lead to the batch grinding equation (6).

$$\frac{dP_i}{dt} = -S_iP_i + \sum_{j=1}^{i-1} b_{ij}S_jP_j \qquad \text{Eq 2}$$

As in any finite difference formulation, the size interval — here the sieve size ratio — must be small enough to define the curvature of the continuous functions. For that reason a complete square-root-of-two sieve series is recommended.

Statement 3 — Breakage functions are not mill-dependent.

The progeny of a particle is invariant, whether it is broken in either a small or a large mill. It is also independent of time and of all operating variables (7). This allows the breakage function to be measured in laboratory mills and then to be used for simulation of industrial mills.

Although this property is theoretically unnecessary, it is of practical importance because it is difficult to study the breakage behavior of particles in production mills. Furthermore, when designing a proposed mill, at least some suppositions must be drawn from laboratory data.

Statement 4 — The residence time distribution is identical for all sizes of particles and is independent of mill operating conditions.

The batch-grinding equation must be integrated over the time that particles remain in the mill. This can be complicated, but the simplifying assumption of Statement 4 provides adequate results for average particles in average mills (8,9).

Studies indicate that the shape of the residence time distribution is of minor concern, provided the average residence time is well known. The average residence time of very large particles may be longer than that of particles of average size. However, coarse particles are usually only a small fraction of the mill load and, therefore, do not significantly affect mill simulation.

Because the shape of the residence time distribution is of minor importance, the curve may be conveniently parameterized by a few constants.

Statement 5 — The absolute selection function (S_iH) is constant in the normal operating range.

The absolute selection function is the absolute mass of material ground per unit time. Experience has indicated that this quantity is independent of operating variables over the *normal* operating range (5). This report confirms this fact.

Summary Statement — Taken together, the above five statements constitute a kinetic ball mill model. The purpose of this report is to validate the model.

Discussion begins with an effort to determine the breakage function from laboratory test data. Next, the role of the residence time distribution is briefly examined. Then, the model is tested using 100 sets of industrial data covering a wide operating range (10,11,12,13). Finally, the identification of possible correlations between operating variables and the absolute selection function is attempted.

2. BREAKAGE FUNCTION DETERMINATION

2.1 LABORATORY GRINDING TESTS

The batch-grinding tests followed SPOC procedures previously published (5), especially for the preparation of special mixtures of single-size fractions. The tests were done on rod mill feed samples collected during sampling campaign numbers 7 and 9 at Brenda Mines in 1977 (11).

The rod mill feed was easy to handle. However, in order to prepare sufficient amounts of material from ball mills in the size fractions of interest, the feed had to be crushed in a dual-roll crusher, which may have introduced anomalous flaws in the particles. To eliminate any possible flaws, the crushed product was placed in the mill and pre-ground for 15 seconds.

Table 1 – Run #7 1977 special feed breakage test results

		Weight per cent retained on size			
Mesh	Size (μm)	Feed	1.5-min product	3.0-min product	(repeat)
8	2400				
10	1700	31.4	14.5	8.6	8.6
14	1200	56.3	38.9	26.4	26.5
20	850	11.7	22.5	22.7	23.3
28	600	0.3	9.4	13.8	13.9
35	425	0.1	4.4	7.7	7.7
48	300	0.1	3.1	5.8	5.5
65	212	0	2.2	4.2	4.6
100	150	0	1.2	2.5	2.4
150	106	0	0.8	1.9	1.8
200	75	0	0.7	1.5	1.3
270	53	0	0.7	1.5	1.3
−270	−53	0.1	1.6	3.4	3.1
14	1200	1.4			
20	850	49.0	26.0	14.5	
28	600	45.3	40.0	32.0	
35	425	4.3	15.0	19.3	
48	300	0	6.9	11.7	
65	212	0	4.2	7.4	
100	150	0	2.2	4.0	
150	106	0	1.5	2.9	
200	75	0	1.1	2.0	
270	53	0	1.0	1.8	
−270	−53	0	2.1	4.4	
28	600	2.7			
35	425	43.1	28.8	19.2	
48	300	45.7	41.8	36.3	
65	212	8.5	16.5	21.1	
100	150	0	4.4	7.6	
150	106	0	2.4	4.5	
200	75	0	1.6	3.1	
270	53	0	1.4	2.6	
−270	−53	0	3.1	5.6	
48	300	1.0			
65	212	54.9	43.6	35.8	
100	150	39.7	38.1	36.6	
150	106	3.4	8.8	11.4	
200	75	0.3	3.1	5.0	
270	53	0.3	2.2	3.8	
−270	−53	0.4	4.2	7.4	

The milling conditions for all the tests were as follows:

Mill - 16.5-cm smooth steel shell, 29 cm in diameter;

Ball charge - 15.52 kg of 2.5-cm cast iron;
- 6.54 kg of 1.9-cm cast iron;
- 1.94 kg of 1.2-cm cast iron (bulk ball volume 40% of mill volume, approximately equal numbers of each size);

Ore charge - 2.500 kg (filled ball void volume);

Mill speed - 57 rpm (73% critical).

The special feed ore charges were dry ground for 1.5 minutes, then removed for size distribution analysis. After analysis, the mill product was replaced, ground for a further 1.5 minutes, and again removed for size distribution analysis. Tables 1 and 2 list the results.

Additional test data were available for rod mill discharge samples collected during a sampling campaign at Brenda Mines in 1981 (5). The tests were done under conditions similar to those described above, except the samples were ground for 2.0 minutes instead of for 1.5-minute intervals. Table 3 lists the results.

Table 2 – Run #9 1977 special feed breakage test results

	Weight per cent retained on size		
Size (μm)	Feed	1.5-min product	3.0-min product
2400			
1700	36.8	17.1	9.0
1200	56.7	40.4	27.7
850	6.1	19.4	21.3
600	0.2	8.5	13.3
425	0.1	4.3	7.6
300	0.1	2.9	5.8
212	0	2.2	4.3
150	0	1.2	2.6
106	0	0.9	1.8
75	0	0.7	1.5
53	0	0.7	1.5
−53	0	1.7	3.6
1200			
850	46.7	23.6	12.9
600	45.0	38.9	29.9
425	7.6	17.1	20.7
300	0.6	7.8	12.6
212	0.1	4.4	7.8
150	0	2.3	4.4
106	0	1.6	3.0
75	0	1.2	2.3
53	0	1.0	2.1
−53	0	2.1	4.3
600			
425	42.8	26.4	17.2
300	45.2	41.7	36.9
212	11.5	18.6	22.0
150	0.5	4.7	7.8
106	0	2.5	4.6
75	0	1.7	3.1
53	0	1.4	2.6
−53	0	3.0	5.8
300	0.5		
212	50.3	40.0	32.5
150	41.9	39.7	37.5
106	4.4	8.8	11.6
75	0.9	3.7	5.4
53	0.8	2.8	4.4
−53	1.2	5.0	8.6

Table 3 – 1981 special feed breakage test results

Size (μm)	Feed	Weight per cent retained on size		
		2.0-min product	4.0-min product	6.0-min product
2400				
1700	62.9	30.5	15.4	
1200	36.7	40.4	34.3	
850	0.2	11.6	15.9	
600	0	6.0	10.4	
425	0	3.0	5.8	
300	0	2.2	4.4	
212	0	1.5	3.1	
150	0	1.1	2.3	
106	0	0.8	1.8	
75	0	0.7	1.7	
53	0	0.5	1.2	
−53	0.3	1.7	3.7	
1200				
850	59.3	33.4	19.4	
600	25.3	30.9	27.3	
425	7.8	14.3	17.5	
300	4.3	8.7	12.0	
212	2.0	5.1	7.6	
150	0.6	2.4	4.4	
106	0.2	1.5	3.0	
75	0.2	1.0	2.5	
53	0	0.7	1.7	
−53	0.2	2.0	4.6	
600	0.8	0.2		
425	47.6	31.0	20.0	
300	32.5	33.4	29.6	
212	10.6	16.4	19.7	
150	5.1	8.4	11.0	
106	3.4	5.4	8.0	
75	0	1.7	3.9	
53	0	1.1	2.5	
−53	0	2.4	5.3	
300	0.1			
212	41.2	28.8	22.5	18.4
150	38.0	38.7	35.6	33.0
106	18.5	21.8	23.0	23.7
75	2.0	5.3	8.0	9.9
53	0.2	1.8	3.5	4.5
−53	0	3.6	7.4	10.4

2.2 ESTIMATING THE BREAKAGE FUNCTION

The breakage function cannot be calculated. However, an *estimated* breakage function can be used in the batch-grinding equation (Eq 2) to calculate a predicted size distribution. Then, the predicted size distribution, **P**, can be compared to the observed size distribution, **P'**, by evaluating the sum of squared residuals, **F**, between the predicted and observed distributions.

$$F = \Sigma[P_i(t) - P'_i(t)]^2 \qquad \text{Eq 3}$$

The sum, F, is called the objective function — because the objective of the program is to minimize the sum of squared residuals by judicious estimation of the breakage function. The estimation procedure is an iterative one using a computer program which tirelessly calculates F for various estimated breakage functions (5).

In performing the laboratory tests, it is assumed that the breakage function measured in the batch mill applies equally to industrial mills. Only the selection (rate) function is mill-dependent. The selection function of the batch mill is of no interest, except for the fact that it is needed to estimate the breakage function.

Theoretically both functions can be simultaneously estimated and this has often been done (14,15). There are three disadvantages to this approach:

1. The batch mill selection function can easily be calculated directly from special feed data without recourse to the breakage function.
2. The computer time required to estimate model parameters increases approximately with the square of the number of parameters. Therefore, using the computer to search for the selection function can significantly increase the computer costs.
3. The results are less accurate because errors in the estimated breakage function can be compensated by errors in the estimated selection function. This leads to good simulation of the laboratory data by entirely incorrect functions. For example, Figure 1 shows a batch mill selection function estimated for the 1981 single-size fraction test results by simultaneous estimation of both the selection and breakage functions. Compare this to the more probable selection function calculated by the simple method explained below.

2.3 CALCULATING THE BATCH MILL SELECTION FUNCTION

To ensure that the correct breakage function is found, the correct batch mill selection function must first be known. The simplest means of determining the selection function is to use Equation 1. If the first-order rate hypothesis is true, then the weight of top size material in a batch-grinding test should decrease logarithmically in time.

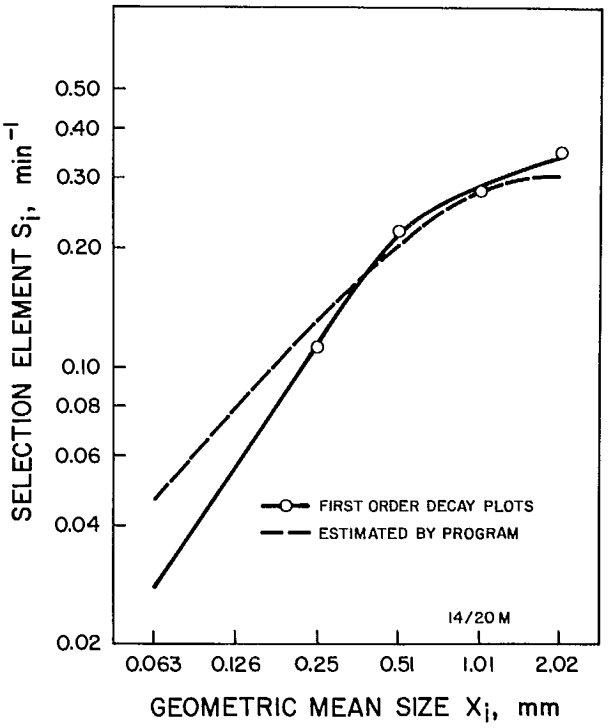

Fig. 1 - Batch mill selection functions — estimated vs calculated

To observe this, note that the general solution of Equation 1 is:

$$P_i(t)/P_i(0) = \exp[-S_i t] \qquad \text{Eq 4}$$

When the logarithm of the weight is plotted as a function of time, the result should be a straight line.

$$\ln[P_i(t)/P_i(0)] = -S_i t \qquad \text{Eq 5}$$

The slope of the line gives directly the selection element, S_i.

Figures 2, 3, and 4 show the first-order decay plots for the batch-grinding test data in Tables 1, 2 and 3. Most of the plots are linear (as hoped) and support the assumption of Equation 1. Therefore, the kinetic model is valid. The minor deviations from linearity may be due to a combination of screening errors, anomalous particle flaws, and preferential grinding of a softer mineral component. These deviations may be safely ignored by using the average slope as the selection element, S_i.

Unfortunately, the pronounced non-linearity of the 48/65 mesh fraction in the 1981 RMD sample (Fig. 4) seriously violates the fundamental assumption of the kinetic model, and any breakage or selection functions estimated from such data would be meaningless.

The decay plot for the 48/65 mesh fraction becomes, however, nearly linear after two minutes. Therefore, some data could be salvaged by treating the two-minute mill product as the mill feed for the next four minutes.

The average slopes of the decay plots in Figures 2, 3, and 4 give only the selection elements of the top size fractions. Some of the remaining elements could be interpolated. However, extrapolation was necessary to find elements for the finest size intervals. The extrapolation was based on a power function, since selection functions often fit power functions (7,14).

$$S_i = a(x_i)^b$$

Or equivalently:

$$\ln(S_i) = \ln(a) + (b)\ln(x_i) \qquad \text{Eq 6}$$

Here $\mathbf{x_i}$ is the geometric mean size of size fraction i; **b** is usually between approximately 0.5 and 1.5; and **a** is dependent on the time scale.

Figure 5 is a plot of $\ln(S_i)$ versus $\ln(x_i)$ for each of the three ore samples. The two 1977 samples have almost identical selection functions, because they are the same ore and were tested under identical conditions.

The 1981 sample resulted in a slightly different selection function, possibly because the ball load, ore load, etc. were slightly different. The functions are markedly curved in the coarse sizes, but the power function does seem to apply to the finer sizes. Even if the extrapolated values are mildly in error, it is not a serious handicap because the breakage function estimation procedure is relatively insensitive to the fine-size selection elements when using coarse single-size fraction data.

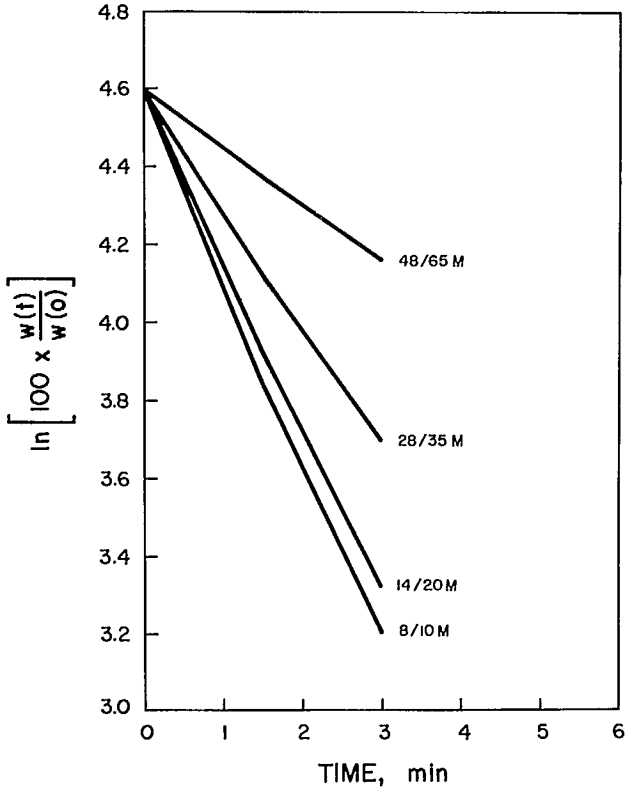

Fig. 3 - First order decay plot — run #9 1977 RMF ore sample

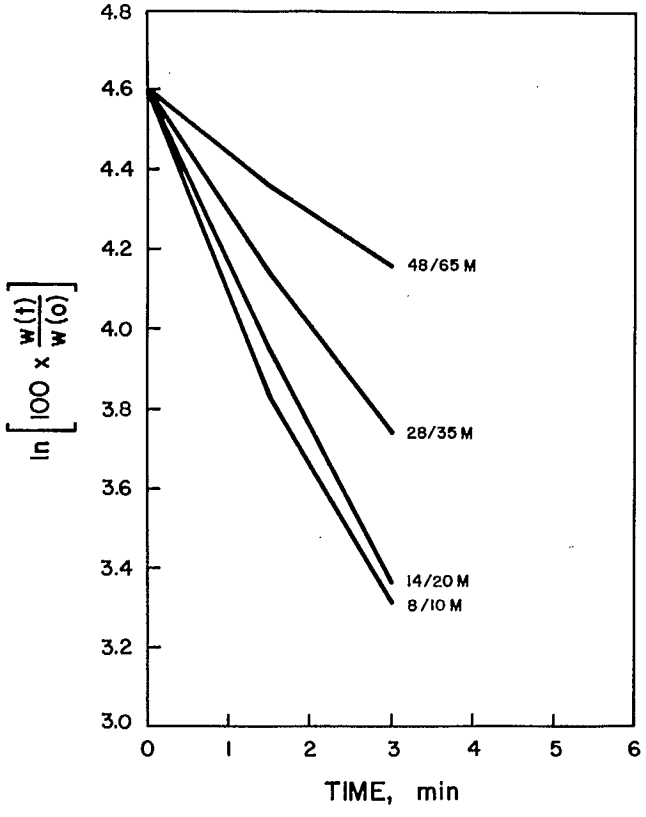

Fig. 2 - First order decay plot — run #7 1977 RMF ore sample

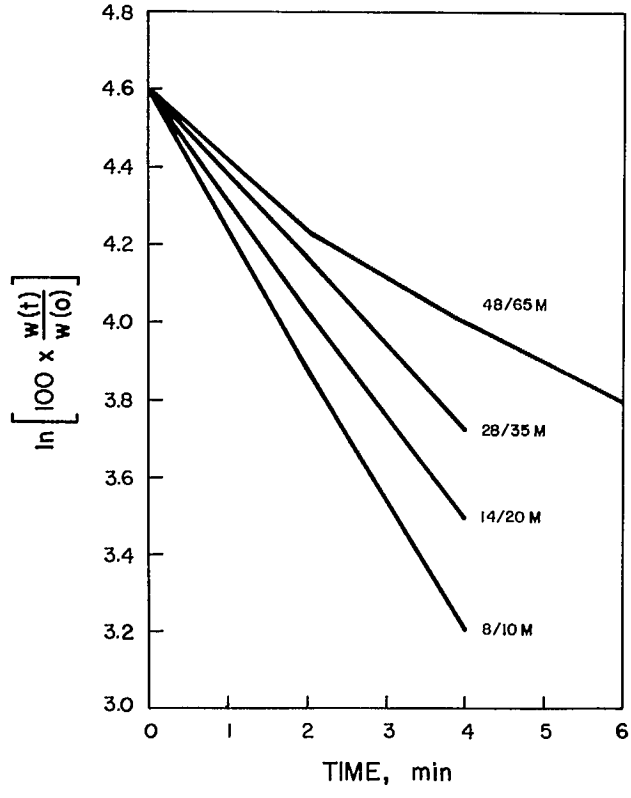

Fig. 4 - First order decay plot — 1981 RMD ore sample

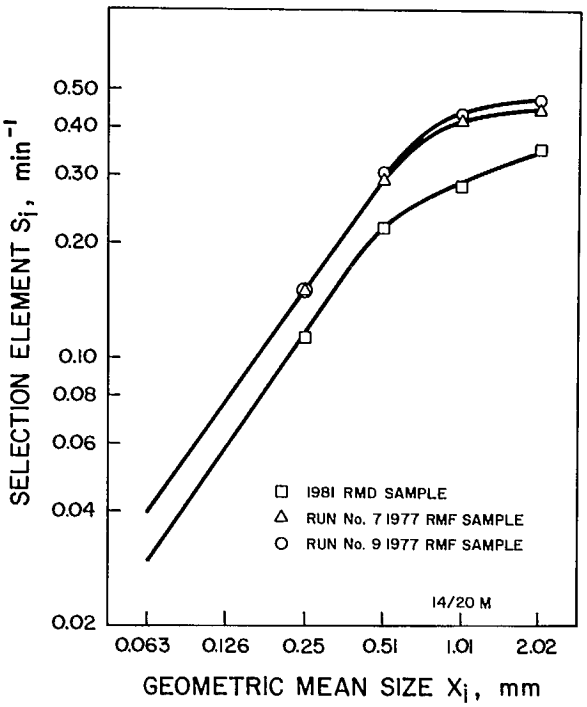

Fig. 5 - Batch mill selection functions — all ore samples

2.4 FORM OF THE BREAKAGE FUNCTION

If there are **n** screen sizes, there are (n-j) breakage elements $\mathbf{b_{ij}}$ for each parent size **j**, and there are **n** parent sizes. It is impractical to estimate all of these elements independently. Instead, it is assumed that the elements fit a smooth function which can be parameterized by a small number of constants, such as b_1, b_2, b_3...

It was assumed that the breakage function was normalized. This means that the size distribution produced by breakage does not depend on absolute particle size, but only on the relative daughter-to-parent size ratio.

The cumulative size distribution has frequently been found to fit the following three-parameter equation (14,15):

$$B_{i,j} = b_1(x_i/x_j)^{b2} + [1-b_1]\,(x_i/x_j)^{b3} \qquad \text{Eq 7}$$

(The breakage elements b_{ij} are calculated as $b_{ij} = B_{i-1,j} - B_{i,j}$).

Later, this restriction was lifted and two non-normalized forms were tried. The first form uses one extra parameter.

$$B_{i,j} = b_1(x_0/x_j)^{b4}(x_i/x_j)^{b2} + [1-b_1(x_0/x_j)^{b4}]\,(x_i/x_j)^{b3} \qquad \text{Eq 8}$$

(x_0 = reference size = 1 mm). The second form used a further two parameters.

$$B_{i,j} = b_1(x_0/x_j)^{b4}(x_i/x_j)^{e1} + [1-b_1(x_0/x_j)^{b4}]\,(x_i/x_j)^{e2} \qquad \text{Eq 9}$$

where:

$e_1 = b_2 + b_5 \ln(x_j)/\ln(R)$

$e_2 = b_3 + b_6 \ln(x_j)/\ln(R)$

R = screen size ratio = .7071

Figure 6 shows a comparison of the estimated cumulative size distributions for the above three functional forms.

The increased flexibility of the non-normalized forms resulted in better predicted size distributions and lower standard errors (see Table 4). More importantly, the extra flexibility minimized the risk that the breakage function would bias the production mill model.

Remember that the ultimate objective of this study is to determine the behavior of production mills selection functions over a range of operating conditions. Unfortunately, the breakage functions themselves can cause significant changes in mill selection functions. This is graphically illustrated in Figures 7 and 8 which compare various production mill selection functions estimated for data collected at Brenda Mines in 1981 (5).

This indicates that the proper selection of a breakage function requires some advance experimentation with the production mill model.

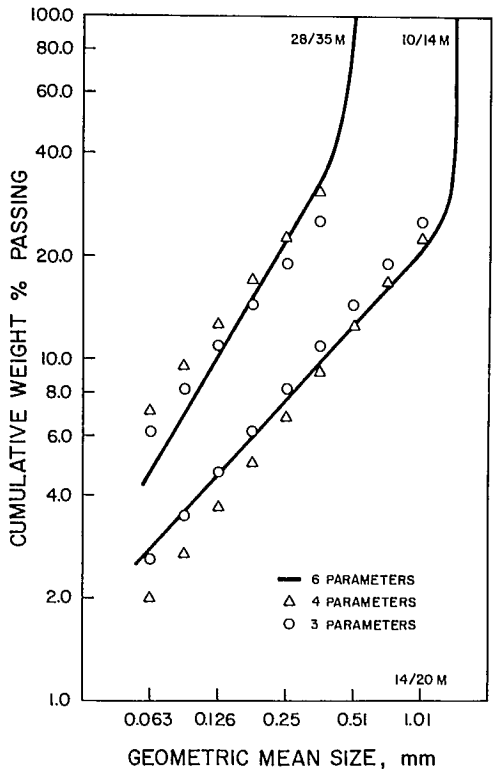

Fig. 6 - Primary breakage distributions — 3, 4, and 6 parameter forms

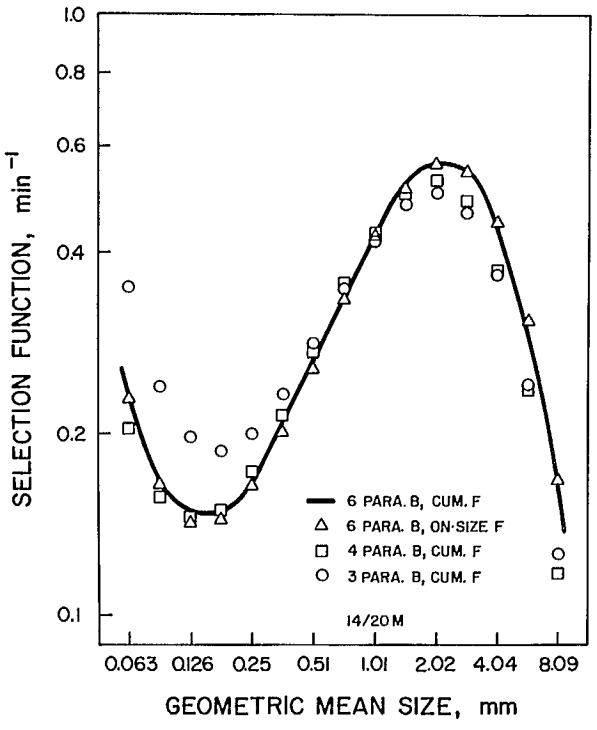

Fig. 7 - Effect of B functional form on cubic selection function

2.5 A NOTE ABOUT OBJECTIVE FUNCTIONS

The minimization of the objective function (Eq 3) is the sole criterion for estimation of the breakage function. Unfortunately, the objective function is poorly understood; for instance, should the objective function compare cumulative per cent passing size distributions or per cent retained on size fractions? What weighting factors should be used? What are the effects of different sieve series?

To illustrate the first question, Figure 9 shows a comparison of breakage functions estimated, using both cumulative and on-size objective functions. It is difficult to know which function is correct. Similarly, Tables 4, 5, and 6 compare various quantities resulting from using cumulative or on-size objective functions. And in Section 4.2, the problem of missing screen sizes is addressed but not satisfactorily resolved.

Because of the lack of firm answers to the above questions, the objective function has usually been with unweighted cumulative per cent passing size distributions. This was done because it frequently resulted in lower objective functions and because cumulative per cent passing values are more meaningful to plant engineers. By not including weighting factors, the magnitude of the pure errors is implicitly assumed to be independent of screen size. Although simple, this is not generally true.

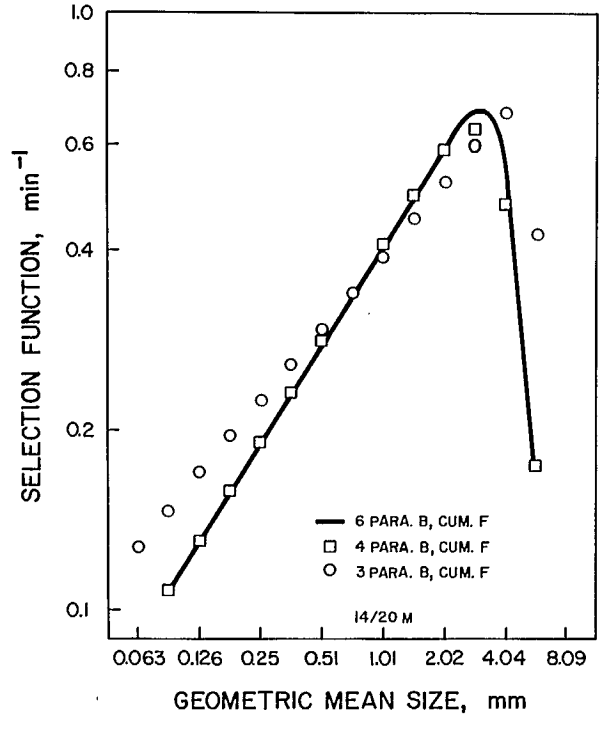

Fig. 8 - Effect of B functional form on hump-*type selection function*

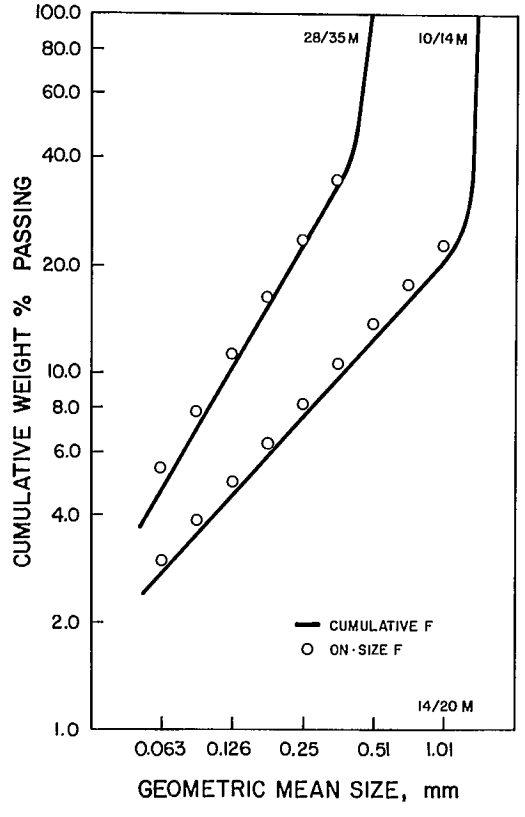

Fig. 9 - Primary breakage distributions — cumulative F vs on-size F

Table 4 – Comparison of breakage functional forms using Table 3 (1981) data

	3 parameter breakage function		4 parameter breakage function		6 parameter breakage function	
	on size F	cum F	on size F	cum F	on size F	cum F
b_1	.3561	.3323	.3678	.3371	.3547	.3317
b_2	.7815	.8035	.9216	.8556	.7347	.7360
b_3	20.00*	20.00*	20.00*	20.00*	20.00*	20.00*
b_4			.3049	.2939	.5140	.5859
b_5					.1157	.1306
b_6					−1.40	−.827
deg. freedom	69	61	68	60	66	58
Obj. func. (F)	141.5	179.8	111.7	84.1	99.2	61.3
Std. error**	1.43	1.72	1.28	1.18	1.23	1.03

*The maximum value of this exponent was limited to 20.00, because greater values are numerically insignificant.
**The standard error is the square root of the objective function divided by the number of measured screen size fractions (not including the pan) minus the number of breakage function parameters, i.e., Std. error = $\{F/(n\text{-}npara)\}^{0.5}$

Table 5 – Effect of B choice on estimated cubic selection function constants

	1981 RMD ore sample				#7 1977	#9 1977
	3-parameter B	4-parameter B	6-parameter B	6-parameter B	6-parameter B	6-parameter B
	cum F	cum F	cum F	on-size F	cum F	cum F
s_1	.4200	.4371	.4307	.4231	.4231	.4291
s_2	.4875	.5433	.6146	.6292	.6204	.6290
s_3	−.2239	−.2777	−.2282	−.2282	−.2282	−.2331
s_4	−.1364	−.1357	−.1357	−.1357	−.1357	−.1343
Std. error	.31	.28	.26	.25	.26	.26

Table 6 – Effect of B choice on estimated *hump*-type selection function constants

	1981 RMD ore sample			#7 1977	#9 1977
	3-parameter B	4-parameter B	6-parameter B	6-parameter B	6-parameter B
	cum F	cum F	cum F	cum F	cum F
s_1	.3898	.4092	.4081	.3966	.4091
s_2	.4023	.5519	.5910	.5623	.5942
s_3	5.792	4.171	3.589	4.227	4.130
s_4	12.48	5.194	5.118	7.331	3.798
Std. error	.51	.35	.53	.50	.50

2.6 COMPARISON OF ORE SAMPLES

The breakage functions calculated from the 1981 and 1977 ore samples are slightly different (see Table 7 and Figure 10). Fortunately, the differences are small and do not lead to large changes in estimated production mill selection functions (Fig. 11 and 12). Nonetheless, the breakage function estimated for the #7 1977 ore sample was chosen as *best*, because it resulted in the lowest objective functions (Table 7). A part of the breakage matrix is shown in Table 8.

It is interesting to note that it is impossible to discriminate between the various breakage functions using only predicted size distributions. Table 9 shows that all the breakage functions produce nearly equivalent product size distributions.

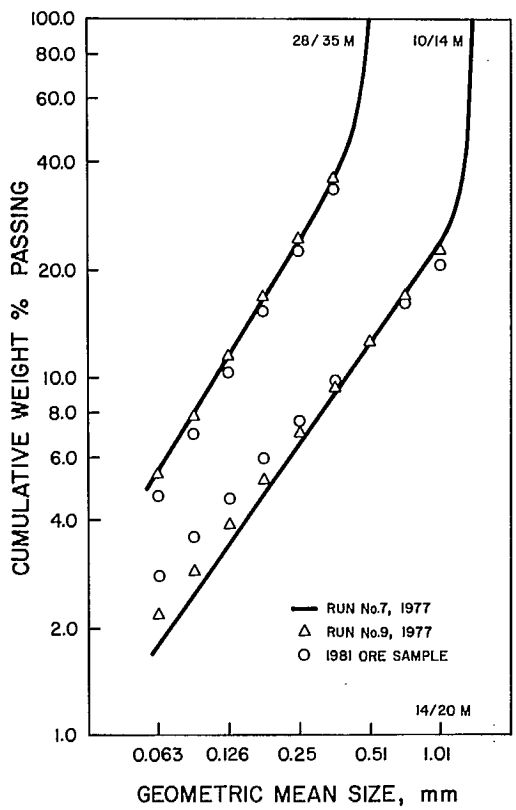

Fig. 10 - Primary breakage distributions — all ore samples

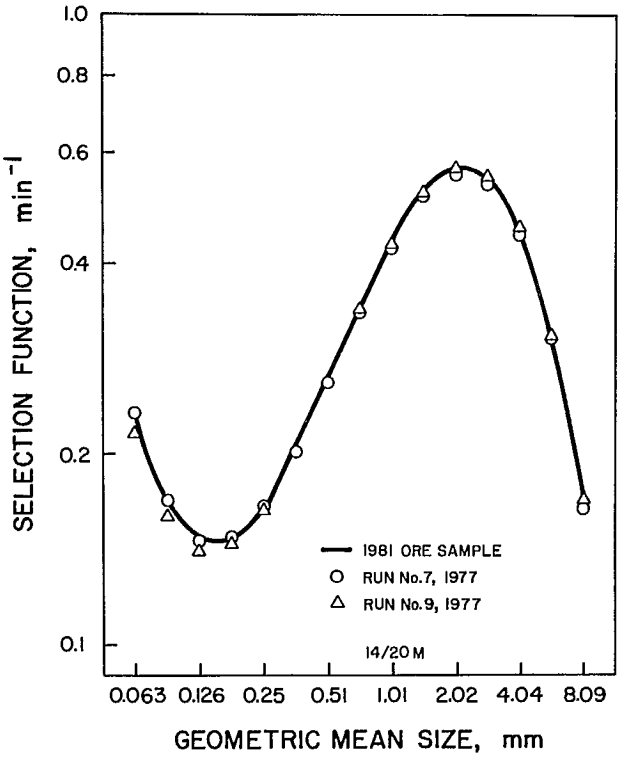

Fig. 11 - Effect of B choice (by ore sample) on cubic selection function

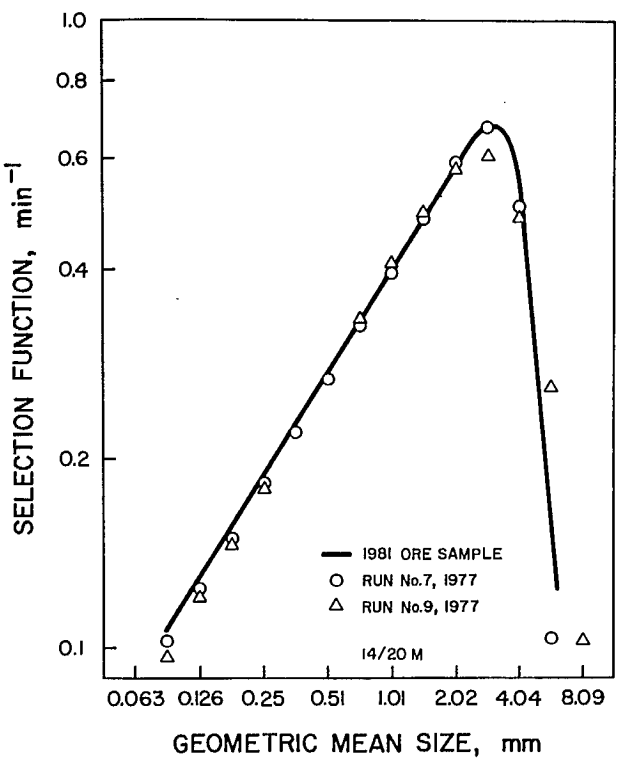

Fig. 12 - Effect of B choice (by ore sample) on hump-*type selection function*

Table 7 – Comparison of estimated breakage parameters

	1981	#7 1977	#9 1977
b_1	.3317	.3786	.3663
b_2	.7360	.9193	.8428
b_3	20.00	14.19	20.00
b_4	.5859	.4138	.5311
b_5	.1306	.0474	.0856
b_6	−.827	−1.93	.5024
Obj. func.	61.3	45.6	46.5
Std. error	1.03	.89	0.90

Table 8 – The *best* breakage distribution matrix (incomplete) – Run #7, 1977

Size (μm)	2400/1700	1700/1200	1200/850	850/600	600/425	425/300	300/212	212/150	150/106
2400/1700	0								
1700/1200	.788	0							
1200/850	.057	.758	0						
850/600	.040	.070	.722	0					
600/425	.030	.047	.085	.678	0				
425/300	.022	.034	.055	.106	.626	0			
300/212	.016	.025	.039	.064	.132	.562	0		
212/150	.012	.018	.028	.045	.075	.165	.485	0	
150/106	.009	.013	.020	.032	.051	.090	.201	.401	0

Table 9 – Effect of B choice on predicted product size distributions

			Predicted product*					
			1981 RMD ore sample				#7 1977	#9 1977
	Experimental (5)		3-parameter B	4-parameter B	6-parameter B	6-parameter B	6-parameter B	6-parameter B
Size (μm)	Feed	Product	cum F	cum F	cum F	on-size F	cum F	cum F
6730	99.9	99.9	99.9	99.9	99.9	99.9	99.9	99.9
4760	99.7	99.8	99.8	99.8	99.8	99.8	99.8	99.8
3360	98.9	99.5	99.5	99.5	99.5	99.5	99.5	99.5
2400	96.1	98.5	98.5	98.5	98.5	98.5	98.5	98.5
1700	92.2	97.3	96.8	96.7	96.7	96.7	96.7	96.7
1200	81.6	91.8	92.3	92.1	92.1	92.1	92.1	92.1
850	69.8	84.2	84.6	84.3	84.2	84.4	84.4	84.3
600	56.3	73.4	73.5	73.2	73.1	73.4	73.4	73.3
425	43.3	61.1	60.5	60.3	60.4	60.8	60.8	60.6
300	31.2	47.8	46.9	47.1	47.4	47.9	47.8	47.7
212	22.8	37.0	35.8	36.4	36.8	37.3	37.1	37.1
150	18.0	29.9	28.2	29.1	29.5	29.9	29.8	29.8
106	14.7	24.5	22.9	24.0	24.1	24.4	24.4	24.4
75	12.1	20.0	19.0	20.1	20.0	20.3	20.3	20.4
53	10.8	17.7	16.6	17.7	17.5	17.8	17.7	17.9
Std. error			.84	.42	.32	.22	.22	.24

*Using *best* selection function (cubic, Table 14) and observed RTD (Brenda, Table 10)

3. RESIDENCE TIME DISTRIBUTIONS

3.1 USE OF RESIDENCE TIME DISTRIBUTION

A residence time distribution is a probability distribution. It is a statistical description of how long particles stay in the mill. For example, consider a mill where 30% of the feed particles leave in less than two minutes, 50% leave between two and five minutes, and 20% leave between five and ten minutes after entering the mill. The residence time distribution of the mill would be as shown in Figure 13.

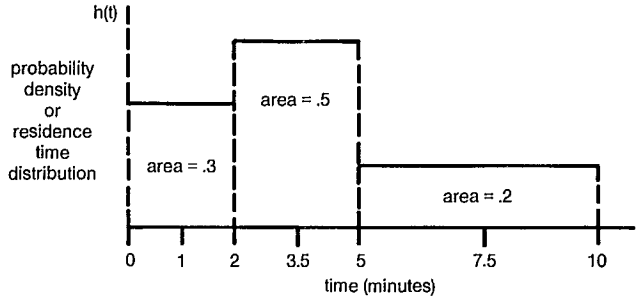

Fig. 13 - A simple residence time distribution

The batch-grinding equation (Eq 2) applies strictly to batch mills and to idealized continuous mills exhibiting only plug flow behaviour. But with the residence time distribution, it can extend to all continuous mills.

A reasonable model might predict the product size distribution P_i^c of a continuous mill as the weighted average of size distributions produced by batch grinding P_i for 1 minute, 3.5 minutes, and 7.5 minutes.

$$P_i^c = 0.3P_i(1\text{ min}) + 0.5P_i(3.5\text{ min}) + 0.2P_i(7.5\text{ min}) = \Sigma[h(t)\,\Delta T]P_i(t)$$

A more exact model would use vanishingly-narrow time intervals (dT), so that the summation becomes an integral (5).

$$P_i^c = \int_{t=0}^{\infty} h(t)P_i(t)dt \qquad \text{Eq 10}$$

This equation implicitly ignores the possibility of different residence time distributions for particles of different sizes. Although this may not be valid in every case, it has been found to be valid for particles of average size in mills operating in the normal range of pulp densities, etc. (8,9).

This equation also assumes, not only that the batch-grinding equation applies as long as particles remain in the mill, but also that the breakage and selection functions do not change as particles move through the mill and grinding progresses.

Again, experience has shown that in most cases these assumptions lead to acceptable mill simulation and, therefore, can be used. For a detailed discussion of residence time distributions, see Chapter 7.3 of the "SPOC Manual" (16).

3.2 THE MIXERS-IN-SERIES MIXING MODEL

The integral in Equation 10 is costly and time-consuming to evaluate. It is more expedient to express the residence time distribution as a simple known function, solve the integral analytically, and calculate only the solution.

From experience it has been found that the most easily integratable functions, which fit observed residence time distributions, are exponential functions of the form xe^{-x}.

Coincidentally, such functions also describe the residence time distributions of perfect-mixers-in-series. Therefore, ball mill models using these functions are said to use a mixing model of perfect-mixers-in-series.

However, this is misleading because the mass transport properties of mills are certainly not those of perfect mixers. It can only be noted that the exponential equations apply and are convenient.

Various authors have used, and been satisfied with, residence time distributions fitted to the following function (7,8,9,17):

$$h(t) = \frac{1}{\theta_1 - \theta_2}\left[\frac{(t/\tau_m - \theta_p)}{\theta_1}\left\{\exp[-(t/\tau_m - \theta_p)/\theta_1]\right\} + \frac{\theta_2}{\theta_2 - \theta_1}\left\{\exp[-(t/\tau_m - \theta_p)/\theta_1]\right\} - \frac{\theta_2}{\theta_2 - \theta_1}\left\{\exp[-(t/\tau_m - \theta_p)/\theta_2]\right\}\right. \qquad \text{Eq 11}$$

This corresponds to the residence time distribution of two perfect mixers θ_1 of equal size, in series with a larger mixer θ_2, as well as a plug flow component θ_p.

The parameter τ_m is the overall average residence time of the mill. This is called a *lumped* parameter model because the flow parameters are lumped into a discrete series of tanks.

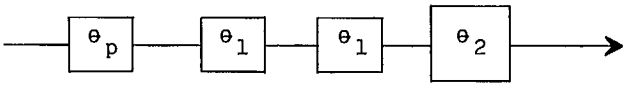

Typical values for the model constants are given in Table 10. The functions generated by those constants are so close to the observed residence time distributions (as determined by tracer tests) that they may be considered representative of the actual observed residence time distributions.

Table 10 – Typical perfect mixers-in-series model constants

	Brenda 1981	Geco 1982
θ_1	0.0973	0.1424
θ_2	0.5597	0.6388
θ_p	0.2457	0.0764
Mill diam (ft)	13.5	12
Mill length (ft)	22	14
% solids	75	74
Feed rate (SDTPH)	847	195

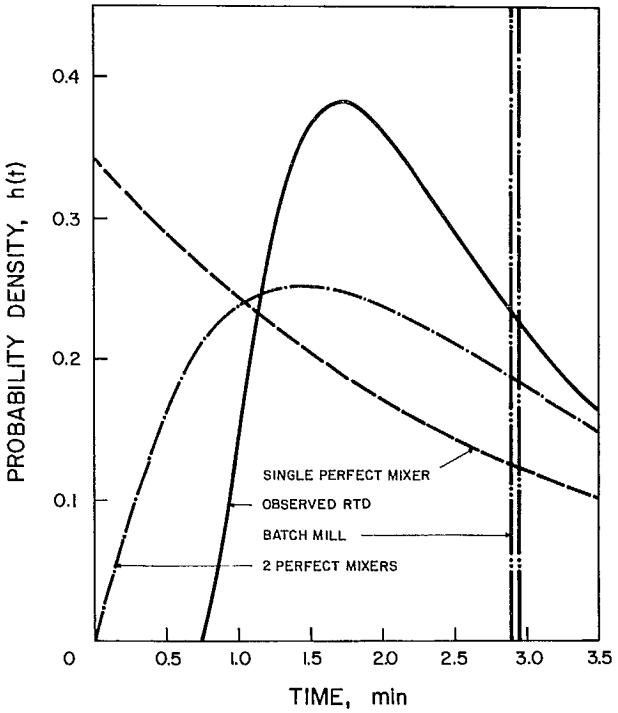

Fig. 14 - Residence time distributions

3.3 EFFECT OF RESIDENCE TIME DISTRIBUTION ON THE MODEL

As Marchand et al. (9), as well as Austin et al., (8) have shown, the product size distribution predicted by Equation 10 is quite insensitive to the shape of the residence time distribution. Therefore, an accurate determination of the residence time distribution is unnecessary.

Table 11 compares the predicted product size distributions using the three different residence time distributions shown in Figure 14 (using data from Reference #5). Notwithstanding gross differences in the residence time distributions, the predicted size distribution is fairly similar. A single perfect mixer residence time distribution appears to be the least adequate, but all the other forms produce results as accurate typical screening errors.

When calibrating a ball mill model, the best residence time distribution should be used. Inaccuracies in the residence time distribution combine with screening errors to generate sizeable fluctuations in the estimated selection function.

Figures 15 and 16, as well as Tables 12 and 13, serve to compare various estimated selection functions. The differences between the functions is of the same order of magnitude as the variations caused by changes in operating variables (Section 4.4). Therefore, to prevent possible bias, use of the three-mixers-in-series-plus-plug-flow model is warranted ("observed RTD" in Figures 15 and 16).

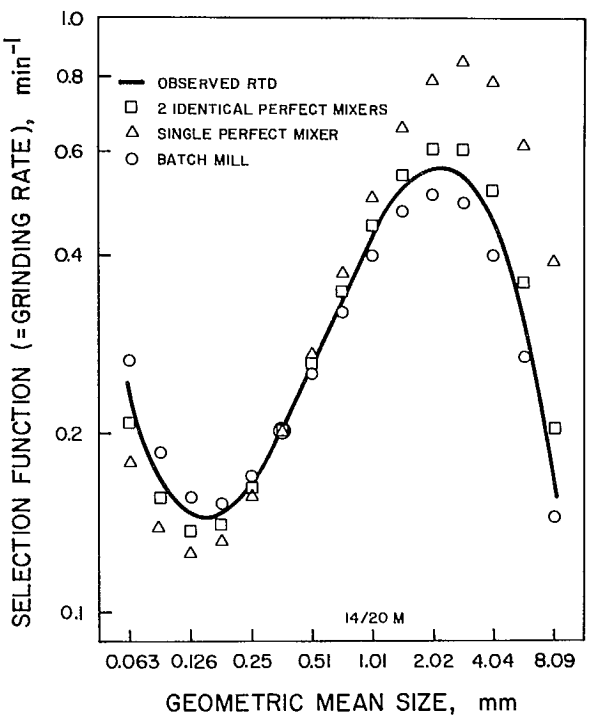

Fig. 15 - Effect of RTD on cubic selection function

Table 11 – Effect of RTD choice on predicted product size distributions (cumulative per cent passing)

	Experimental (5)		Predicted product*			
Size (μm)	Feed	Product	Batch	Single PM	Two PM	Three PM + plug = obs. RTD
6730	99.9	99.9	99.9	99.9	99.9	99.9
4760	99.7	99.8	99.8	99.8	99.8	99.8
3360	98.9	99.5	99.5	99.4	99.4	99.5
2400	96.1	98.5	98.7	98.2	98.4	98.5
1700	92.2	97.3	97.1	96.0	96.5	96.7
1200	81.6	91.8	93.0	90.7	91.7	92.2
850	69.8	84.2	85.5	82.6	83.8	84.4
600	56.3	73.4	74.4	71.7	72.9	73.4
425	43.3	61.1	61.5	59.4	60.4	60.8
300	31.2	47.8	48.2	46.9	47.5	47.7
212	22.8	37.0	37.3	36.7	37.0	37.1
150	18.0	29.9	29.8	29.6	29.8	29.8
106	14.7	24.5	24.3	24.4	24.4	24.4
75	12.1	20.0	20.2	20.5	20.4	20.3
53	10.8	17.7	17.5	18.0	17.8	17.7
Std. error			.55	.89	.33	.22

*Using *best* breakage function (Table 8) and *best* selection function (cubic, Table 14)

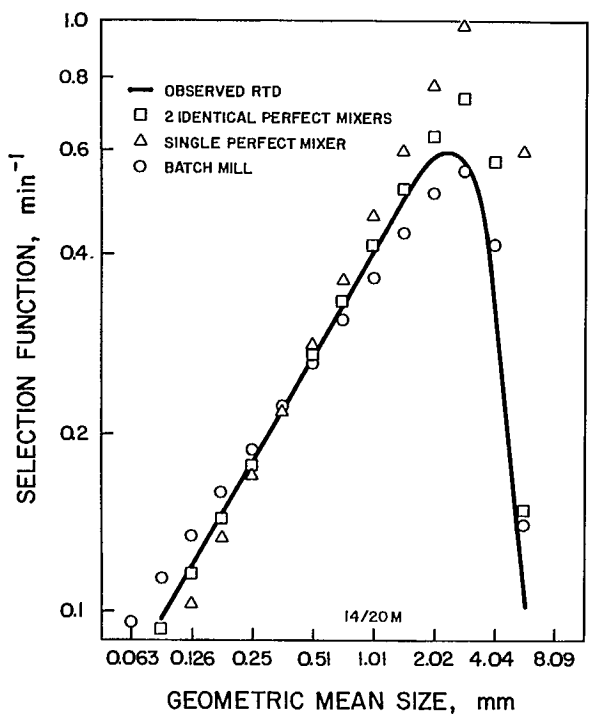

Fig. 16 - Effect of RTD on hump-*type selection function*

Table 12 – Effect of RTD choice on cubic selection function constants

	Batch	Single PM	Two PM	Obs. RTD
s_1	.3971	.4986	.4418	.4207
s_2	.5758	.8330	.6694	.6146
s_3	−.2209	−.1865	−.2211	−.2282
s_4	−.1362	−.1290	−.1321	−.1357
Std. error	.28	.20	.23	.26

Table 13 – Effect of RTD choice on *hump*-type selection function constants

	Batch	Single PM	Two PM	Obs. RTD
s_1	.3696	.4650	.4177	.4081
s_2	.4872	.7263	.6181	.5910
s_3	4.273	75.00	4.276	3.589
s_4	5.614	30.00	6.399	5.118
Std. error	.44	.53	.51	.53

4. PRODUCTION MILL SELECTION FUNCTION DETERMINATION

4.1 ESTIMATING THE PRODUCTION MILL SELECTION FUNCTION

Production mill selection functions cannot be directly calculated. They can only be estimated and used to predict product size distributions that match as closely as possible a measured size distribution. The *best* estimated selection function is the one which results in the lowest sum of squared residuals F in Equation 3. If the measured size distribution is wrong because of sampling or screening errors, then the chosen *best* selection function will also be wrong.

The batch-grinding equations (Eq 2 and Eq 10) are used to calculate product size distributions. In addition to an estimated selection function, these equations also require a breakage function and residence time distribution. If either is incorrect, the sum of squared residuals F will be adversely affected, and an incorrect *best* selection function will be chosen.

In Section 2 a common *best* breakage function (Table 8) was determined from laboratory tests on ore from the Brenda Mines. In Section 3, the residence time distribution of Brenda Mines' ball mill was parameterized (Table 10). Those results are used in this section to estimate selection functions for Brenda Mines' ball mill. Throughout the development, the various assumptions underlying the estimation procedure should be kept in mind.

The simplest selection functions fit a power function similar to a Schuhmann distribution (7).

$$S_i = s_1(x_i/x_0)^{s_2} \qquad \text{Eq 12}$$

Or equivalently:

$$\ln(s_i) = \ln(s_1) + s_2 \ln(x_i/x_0)$$

where x_0 = 1mm

However, this equation does not have sufficient flexibility to fit most observed selection functions. Therefore three extensions were tried.

The Quadratic

$$\ln(S_i) = \ln(s_1) + s_2 \ln(x_i/x_0) + s_3 [\ln(x_i/x_0)]^2 \qquad \text{Eq 13}$$

The Cubic

$$\ln(S_i) = \ln(s_1) + s_2 \ln(x_i/x_0) + s_3 [\ln(x_i/x_0)]^2 + s_4 [\ln(x_i/x_0)]^3 \qquad \text{Eq 14}$$

The Hump or Modified Schuhmann

$$S_i = \frac{s_1(x_i/x_0)^2}{1 + [(x_i/x_0)/s_3]^{s4}} \qquad \text{Eq 15}$$

These equations were fitted to the selection function of a sampling campaign at Brenda Mines in 1981. Table 14 gives the constants which resulted in the minimum objective functions. The estimated selection functions are shown graphically in Figure 17. Finally, Figure 18 shows a comparison of the respective product size distributions.

Table 14 – Comparison of estimated selection function constants

	Schuhmann	Quadratic	Cubic	*Hump*
s_1	.3929	.3868	.4207	.4081
s_2	.5592	.5924	.6146	.5910
s_3		.04043	−.2282	3.589
s_4			−.1357	5.118
Obj. function	3.31	3.00	.817	3.31
Deg. freedom	15-2	15-3	15-4	15-4
Std. error	.49	.48	.26	.53

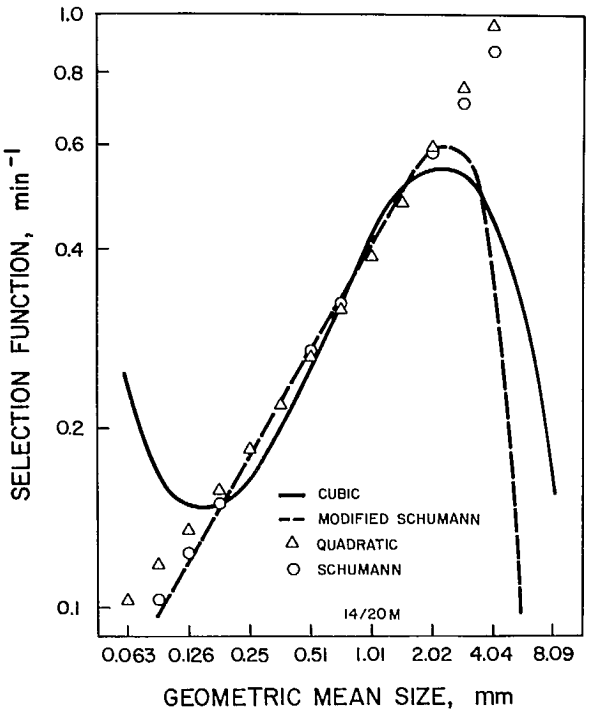

Fig. 17 - Comparison of selection functional forms

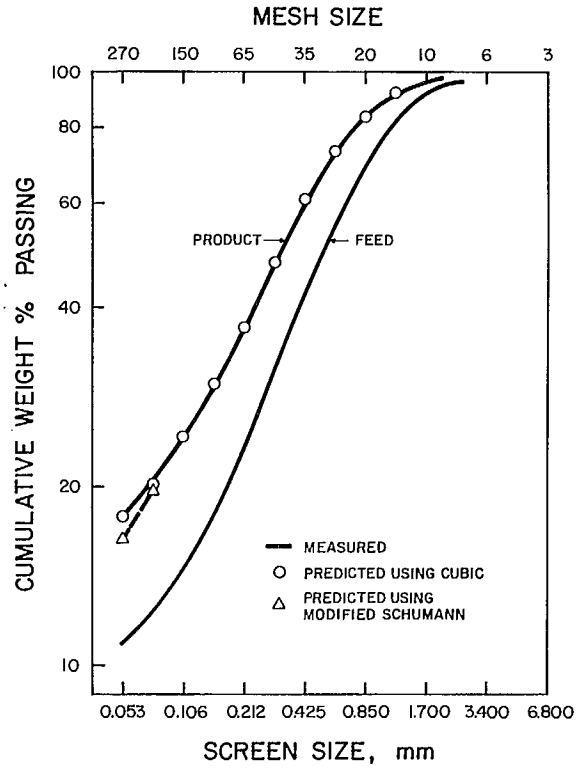

Fig. 18 - Comparison of product size distributions

All four types of selection functions simulate the predicted product size distribution admirably. The simplest type, the power or Schuhmann distribution, worked well for the medium-sized particles, but is too inflexible to predict perfectly the observed size distribution in the very-coarse and very-fine size ranges. The quadratic is a slight improvement, but not enough to be significant. The *hump* or modified Schuhmann equation permits reduced grinding rates in the coarse sizes which allowed it to predict the coarse size fractions better than the simple Schuhmann.

However, in terms of the standard deviation of residuals, the modification provides no real advantage because the reduction in the sum of squared residuals is not enough to compensate for the additional two parameters.

The cubic is far superior to other forms. Unfortunately, although selection functions have frequently been observed to deviate from simple power functions (18,19), it is difficult to explain why the grinding rate would increase as particle size decreases below 100 mesh. One can speculate about possible causes:

- A large fraction of soft material between 150 and 270 mesh could elevate the grinding rate for those sizes.
- A large fraction of hard material between 65 and 100 mesh depresses the grinding rate there. Perhaps the action of the mill is exceptionally effective for 150/270 mesh particles.
- Invalid model assumptions or data lead to this curiosity; for instance, the measured product size distribution could be in error.

Most of the differences between predicted and measured distributions occur in the finest two-size intervals. Unfortunately, Figure 18 shows that the measured distribution would have to be seriously in error to meet the size distribution predicted by a selection function fitted to a Schuhmann or *hump*-type equation. Only the cubic equation has the flexibility to predict the observed size distributions.

As a final note, it must be pointed out that the calculation of the constants in Table 14 is subject to some uncertainty. Different initial estimates of the constants lead to different final values. In some cases, particular sets of constants provide lower objective functions than other sets of constants, and so the better sets were chosen.

However, in other cases, two or more quite different sets of constants result in very comparable objective functions. Perhaps the objective function surfaces are very flat near the minima, and so the stopping point depends on the step size, on the approach direction, and even possibly on the search method.

4.2 EFFECT OF MISSING SCREEN SIZES

Size distribution data for the 1975 Brenda sampling campaigns are available only for a 2:1 geometric sieve series (10). Data for the 1977 campaigns were recorded on an incomplete square root of two sieve series (11). As mentioned in Section 2.5, the sieve series is closely linked with other questions about the objective function. Therefore, it was thought necessary to study the effects of missing screen sizes.

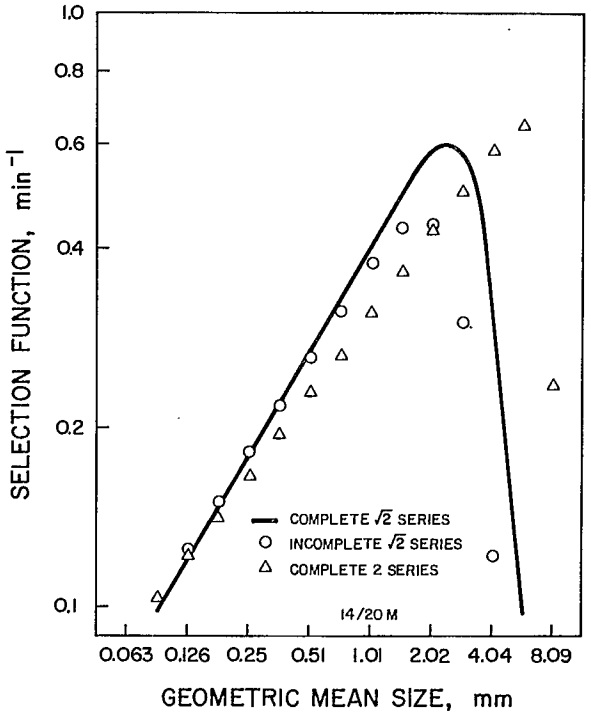

Fig. 19 - Effect of sieve series on **hump-type selection function**

In any discrete size analysis the properties of all particles in a size fraction are lumped together and averaged. If the size interval is too large to discriminate important changes in the properties of the particles, then serious calculation errors are introduced.

When narrow-size fraction data are not available, the effect of interval averaging can be somewhat negated by doing all calculations on narrow-size fractions, and then using an abbreviated objective function which includes only the measured-size fractions. Unfortunately, Figure 19 shows that even this approach can lead to serious mistakes in the estimation of the selection function.

The procedure is most inadequate in the coarse size fractions where the cumulative size distribution is nearly constant. Normally with a square root of two sieve series, the coarse sizes contribute little to the objective function. In a reduced sieve series, it becomes practically impossible to estimate the selection function in the coarse sizes. Therefore, it was deemed necessary to interpolate the missing screen sizes by plotting the cumulative size distribution for the 1975 and 1977 sampling campaign data. Then, at least the objective functions would be comparable.

4.3 EFFECT OF NOT KNOWING THE AVERAGE RESIDENCE TIME

The average residence time must be accurately known to estimate the selection function. Unfortunately, the average residence times were not measured for the 1975 and 1977 sampling campaigns. However, the feed rates Q were measured, therefore the absolute selection function S_iH can be calculated. This corresponds to calculating the amount of material ground without knowing how much was in the mill, or how long it stayed in the mill.

In 1981 the residence time distribution h(t) of Brenda Mines' mill was measured. The model constants are given in Table 10.

When τ_m is not known, a new variable $\gamma = t/\tau_m Q$ can be defined.

By substituting $t = \gamma \tau_m Q$ into Equation 11, the variable τ_m is eliminated. The new distribution $h(\gamma)$ can then be used in Equation 10 which does not change when a different dummy variable is used.

$$P_i^c = \int_{\gamma=0}^{\infty} h(\gamma) P_i(\gamma) d\gamma \qquad \text{Eq 16}$$

But remember that $P_i(t)$ is calculated from the batch-grinding equation, which must now be modified to be a function of γ instead of t.

$$\frac{dP_i(t)}{dt} = \frac{dP_i(\gamma)}{\tau_m Q d\gamma} = -S_i P_i + \sum_{j=1}^{i-1} b_{ij} S_j P_j$$

$$\frac{dP_i(\gamma)}{d\gamma} = -(S_i \tau_m Q) P_i + \sum_{j=1}^{i-1} b_{ij} (S_j \tau_m Q) P_j$$

$$= -\bar{S}_i P_i + \sum_{j=1}^{i-1} b_{ij} \bar{S}_j P_j \qquad \text{Eq 17}$$

Now Equations 16 and 17 can be used to estimate $\bar{S}_i$ just as Equations 2 and 10 were used to estimate S_i.

The quantity $\bar{S}_i = (S_i \tau_m Q)$ is best interpreted by noting that: $\tau_m = H/Q$ where H is the mill holdup mass. Therefore, $\bar{S}_i = S_i H$. It is called the absolute selection function because it represents the absolute mass ground per unit time.

4.4 EFFECT OF OPERATING VARIABLES

A quantitative knowledge of S_iH is crucial to predicting mill performance. Therefore, an attempt was made to detect the possible effects of operating variables on S_iH.

Absolute selection functions were calculated for all 47 sets of sampling campaign data collected at Brenda Mines in 1975 and 1977. To compare the functions they were scaled by the factor $1/H_0$, where H_0 is the holdup mass calculated from the 1981 sampling campaign and residence time distribution data (5). If the holdup mass were constant, this scaling would result in the actual selection function S_i.

Tables 15 and 16 contain the parameters for the *hump*-type selection functions which minimized the sum of squared residuals. If S_iH were affected by changes in the feed rate Q, pulp per cent solids %S or feed size distribution %-65M, then the parameters of the selection function should, in some way, be correlated to those variables. For instance, plots of S_1H/H_0 versus feed rate might show some trend. However, there are no reliable correlations between any of the variables in Tables 15 and 16.

The fact that the variable S_iH/H_0 is not correlated to operating variables does not mean that the mill holdup does not change with operating parameters. It only means that, if H changes, then S_i changes inversely to negate any potential change in the product S_iH.

This result has an important interpretation. It indicates that the absolute selection function, S_iH, or the mill grinding capacity does not change with changes in operating variables over the normal operating range. The mill product can be adjusted by altering the feed rate, but the total amount of grinding remains constant.

If the absolute selection function is not correlated to operating variables, then a single absolute selection function should apply to all data sets. The hypothesis was tested by calculating predicted size distributions for all 47 runs using the average function parameters from Tables 15 and 16.

The column labelled SE_m in the tables shows that the standard error per screen remained below 1% in most cases. This is less than the standard deviation calculated for the measured distributions from replicate runs (11). Moreover, the standard errors (model residuals) are not correlated to the operating variables or time. For example, in Figures 20 and 21 the standard errors are plotted against feed rate, and in Figure 22 the standard error is plotted against run sequence.

Table 15 – Estimated selection function parameters — 1975 data

Run	$s_1 H/H_0$	s_2	s_3	s_4	Q(SDTPH)	%S	%-212 μm	SE_b**	SE_m***
1	.342	.603	5.88	9.74	733	75.62	25.1	.86	.85
2	.361	.641	16.0*	10.0*	817	75.59	21.3	.93	.84
3	.370	.695	16.0*	10.0*	838	75.50	23.7	.82	.71
4	.360	.725	5.14	7.80	885	76.12	21.9	.77	.80
5	.390	.800	4.97	10.0*	655	70.45	25.1	.73	.75
6	.388	.650	4.42	5.15	849	75.15	22.2	.76	.87
7	.384	.731	4.90	10.0*	591	72.70	24.4	1.0	.88
8	.418	.796	3.61	5.43	756	74.69	23.9	.53	.64
9	.371	.678	4.10	7.29	906	74.30	26.7	.64	.57
10	.389	.794	5.14	5.91	988	75.84	24.9	.48	.48
11	.392	.793	3.09	7.21	909	74.26	26.5	.53	.53
12	.355	.685	4.34	5.27	885	75.70	24.4	.64	.68
13	.387	.804	16.0*	10.0*	692	71.08	24.8	.88	.89
14	.402	.729	3.83	5.25	788	75.77	23.0	.46	.57
15	.350	.653	6.55	7.41	697	73.50	22.6	.74	.73
16	.388	.755	4.82	4.80	839	74.56	21.2	.65	.58
17	.413	.776	4.24	5.31	889	74.19	25.8	.65	.68
18	.379	.689	4.01	5.30	860	76.31	23.3	.73	.66
19	.401	.693	3.75	4.56	791	76.30	22.8	.65	.79
20	.381	.809	3.36	3.26	930	75.88	18.8	.25	.61
df	19	19	16	14	19	19	19	19	19
Avg	.381	.725	4.48	5.98	815	74.67	23.6	.68	.71
SD	.020	.064	0.90	1.61	102	1.73	2.0	.18	.13

*Maximum permitted value

**SE_b = standard error using a variable four-parameter selection function = $[\Sigma(P-M)^2/10]^{0.5}$

where P = predicted cumulative per cent passing
M = measured cumulative per cent passing
10 = (14 screens — 4 adjustable parameters)

***SE_m = standard error using a constant selection function = $[\Sigma(P-M)^2/14]^{0.5}$

Table 16 – Estimated selection function parameters — 1977 data

Run	s_1H/H_0	s_2	s_3	s_4	Q(SDTPH)	%S	%–212 μm	SE_b**	SE_m***
1	.440	.805	4.31	10.0*	651	68.17	31.7	.37	.88
2	.412	.708	4.80	8.65	694	69.65	27.2	.38	.62
3	.368	.652	3.30	10.0*	667	71.83	23.0	.61	1.3
4	.431	.635	4.85	4.69	880	73.02	25.4	.38	.64
5	.437	.627	3.83	3.56	876	72.51	24.0	.33	.66
6	.415	.495	6.02	6.34	997	76.72	18.5	.42	.96
7	.416	.878	3.68	10.0*	558	65.17	32.3	.58	2.1
8	.380	.670	16.0*	10.0*	672	70.01	25.0	.59	1.1
9	.348	.582	16.0*	10.0*	679	70.90	23.2	.62	1.3
10	.412	.583	6.54	6.85	845	72.26	22.9	.43	.56
11	.405	.515	4.78	8.25	1002	74.18	20.3	.44	.71
12	.397	.698	4.80	2.82	636	69.43	28.6	.53	.84
13	.392	.694	5.33	7.06	693	70.88	26.8	.69	.98
14	.394	.619	5.60	10.0*	804	70.64	24.9	.79	.70
15	.411	.570	4.47	4.09	873	73.38	25.0	.34	.52
16	.394	.528	5.94	3.67	857	74.08	22.7	.61	.68
17	.388	.635	4.30	2.85	919	75.89	20.1	.26	.67
18	.374	.541	6.35	7.98	778	74.28	21.7	.51	.61
19	.377	.661	3.98	4.67	634	71.13	25.3	.35	1.1
20	.370	.589	16.0*	10.0*	678	70.30	23.8	.59	.81
21	.404	.609	4.30	4.09	834	73.18	23.9	.48	.44
22	.396	.470	6.62	6.87	1073	75.67	17.5	.44	.78
23	.388	.491	4.68	4.33	1277	72.27	22.4	.29	.52
24	.379	.500	5.59	7.70	1683	71.21	23.4	.33	.39
25	.432	.606	5.40	8.49	861	73.64	21.8	.64	.94
26	.439	.695	5.09	10.0*	570	74.09	23.7	.73	.82
27	.422	.492	3.91	4.09	1088	74.93	19.0	.36	.99
df	26	26	23	18	26	26	26	26	26
Avg	.401	.613	4.94	5.64	843	72.20	23.9	.48	.84
SD	.024	.098	0.93	2.03	240	2.56	3.5	.14	.35

*Maximum permitted value

**$SE_b = [\Sigma(P-M)^2/10]^{0.5}$

***$SE_m = [\Sigma(P-M)^2/14]^{0.5}$

Table 17 shows that about 99% of the variation on any screen was explained by the simple model (columns entitled "modl") using a constant absolute selection function.

The impressive power of the simple model to mimic measured results is graphically shown in Figures 23 through 26. This proves that the simple model is adequate and explains all significant variation in the observed size distributions.

Finally, Tables 18 and 19 show a breakdown of the standard error for each screen size. In the 1977 data set, the simple model seemed to do most poorly in the finest screen sizes. This resulted from accumulated errors, because the size distributions were expressed on a cumulative *per cent passed* basis. When restated on a *per cent retained* basis, the model predicted equally well in the coarse and fine sizes.

In both the 1975 and 1977 data sets, the errors in the pan fractions (-270 M) were greater than any other sizes. Furthermore, the predicted pan fractions were always less than the measured pan fractions. This is a direct result of using the *hump*-type selection function.

Figure 18 compares a typical example of a measured-size distribution and that predicted by a model using a *hump*-type selection function.

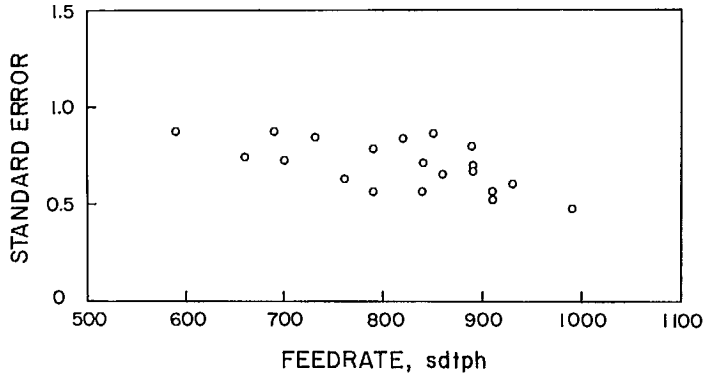

Fig. 20 - Standard error vs feed rate — 1975 data

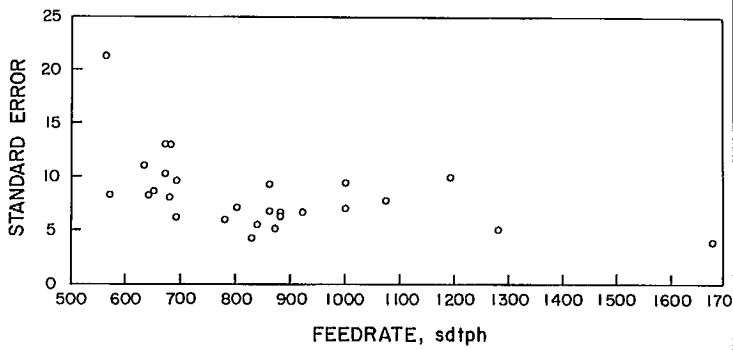

Fig. 21 - Standard error vs feed rate — 1977 data

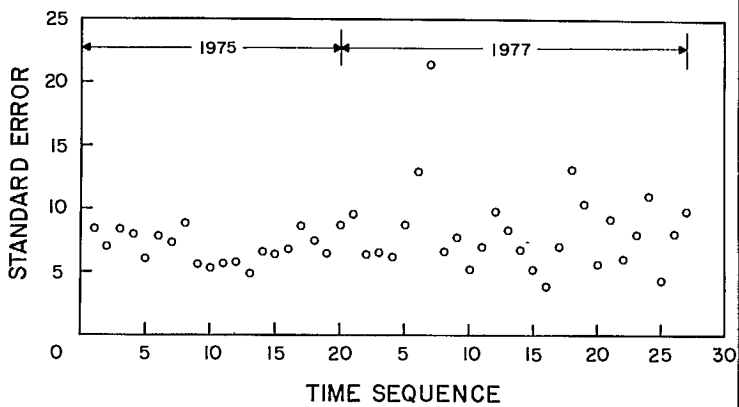

Fig. 22 - Standard error vs run sequence — 1975 and 1977 data

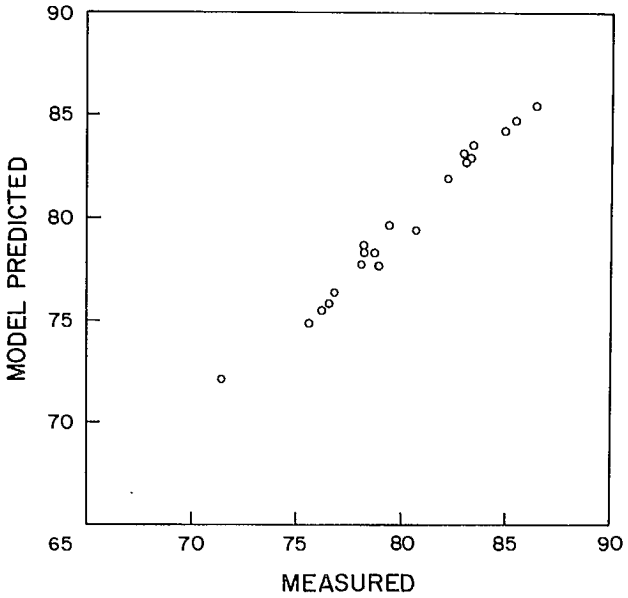

Fig. 23 - −28 mesh predicted vs measured — 1975 data

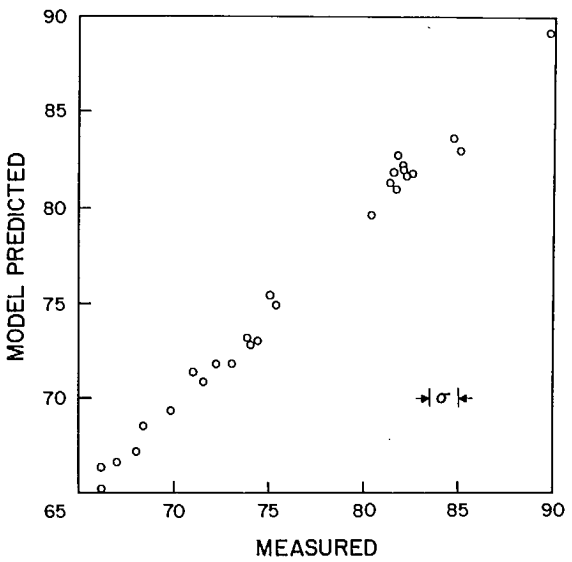

Fig. 25 - −28 mesh predicted vs measured — 1977 data

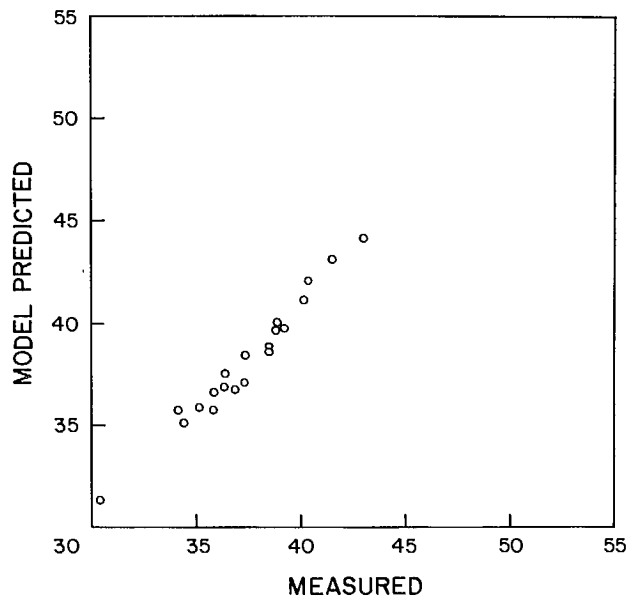

Fig. 24 - −65 mesh predicted vs measured — 1975 data

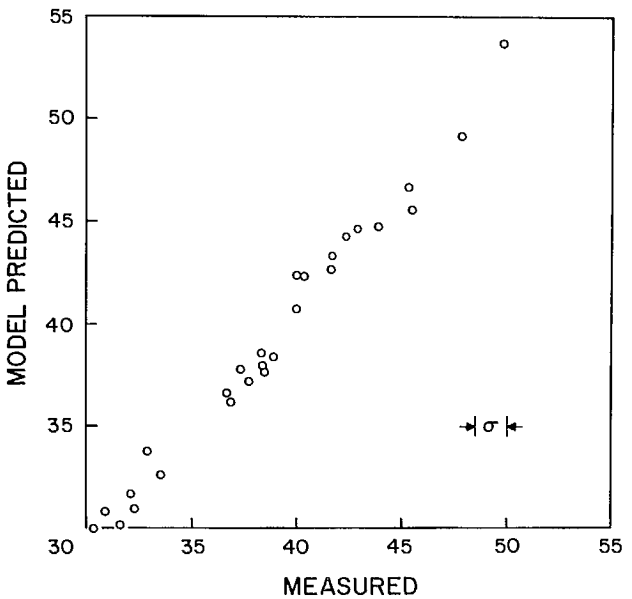

Fig. 26 - −65 mesh predicted vs measured — 1977 data

Table 17 – Correlation coefficients by screen — 1975 and 1977 data

	1975 campaigns				1977 campaigns			
	Cumulative		On-size		Cumulative		On-size	
Size (μm)	Best	Modl	Best	Modl	Best	Modl	Best	Modl
6730	.976	.970	.976	.970	.791	.960	.791	.960
4760	.959	.966	.945	.951	.897	.988	.653	.977
3360	.976	.958	.968	.947	.948	.968	.862	.898
2400	.948	.887	.849	.750	.994	.986	.986	.979
1700	.992	.982	.952	.979	.998	.990	.990	.984
1200	.995	.990	.988	.985	.998	.992	.991	.988
850	.998	.991	.994	.977	.999	.994	.998	.992
600	.999	.991	.995	.987	1.000	.995	.987	.975
425	1.000	.992	.987	.979	.999	.992	.955	.851
300	.999	.998	.963	.956	1.000	.991	.968	.848
212	.997	.982	.998	.987	1.000	.990	.989	.961
150	1.000	.976	.976	.956	1.000	.988	.990	.989
106	.999	.968	.956	.942	.999	.985	.987	.984
75	.993	.962	.923	.912	.998	.983	.958	.951
53	.980	.955	.790	.748	.992	.979	.942	.992

Note: The correlation coefficient used here is the normalized covariance. It is employed because both the predicted and measured product size distributions were subject to error (20).

$$r = \frac{\text{cov(predicted, measured)}}{[\text{var(predicted)var(measured)}]^{0.5}} = \frac{\Sigma(P-\bar{P})(M-\bar{M})}{[\Sigma(P-\bar{P})^2\ \Sigma(M-\bar{M})^2]^{0.5}}$$

Table 18 – Standard error breakdown by screen — 1975 data

	Cumulative								On-size		
	Average size distribution				Standard variation**				Standard error***		
Size (μm)	Feed	Dis.	Best	Modl	Feed	Dis.	Best	Modl	Best	Modl	Modl
6730	100.0	100.0	100.0	100.0	.0	.0	.0	.0	.0	.0	.0
4760*	99.7	99.9	99.8	99.8	.2	.1	.1	.1	.1	.1	.1
3360	99.4	99.8	99.7	99.7	.3	.2	.2	.2	.1	.1	.0
2400*	97.6	99.1	99.3	99.4	1.1	.4	.4	.3	.3	.3	.4
1700	93.9	97.8	98.0	98.1	2.0	1.0	.9	.8	.3	.4	.3
1200*	88.3	95.3	95.1	95.1	3.0	1.7	1.6	1.6	.3	.3	.6
850	79.1	89.8	89.3	89.4	3.9	2.6	2.6	2.6	.5	.6	.3
600*	65.8	80.0	79.6	79.7	4.7	3.9	3.7	3.8	.4	.6	.3
425	50.8	66.9	66.6	66.6	4.5	4.5	4.3	4.4	.4	.6	.2
300*	35.0	50.8	51.5	51.5	3.0	3.7	3.8	3.9	.7	.9	1.1
212	23.6	37.4	38.2	38.7	2.0	2.9	3.0	3.0	.9	1.0	.2
150*	16.9	28.3	28.7	28.7	1.4	2.4	2.4	2.4	.5	.7	.4
106	12.6	21.9	21.9	21.9	1.2	2.1	2.1	2.0	.1	.5	.6
75*	9.9	17.7	16.9	17.0	1.1	1.9	1.8	1.7	.8	.9	.7
53	8.3	15.1	13.4	13.4	1.0	1.7	1.5	1.5	1.7	1.8	1.0

* Interpolated data

**Standard variation = $[\Sigma(M-\bar{M})^2/19]^{0.5}$ or $[\Sigma(P-\bar{P})^2/19]^{0.5}$

***Standard error = $[\Sigma(P-M)^2/19]^{0.5}$

Table 19 – Standard error breakdown by screen — 1977 data

	Cumulative								On-size		
	Average size distribution				Standard variation**				Standard error***		
Size (μm)	Feed	Dis.	Best	Modl	Feed	Dis.	Best	Modl	Best	Modl	Modl
6730	99.9	99.9	99.9	99.9	.1	.1	.1	.1	.1	.0	.0
4760	99.6	99.8	99.8	99.9	.3	.2	.2	.1	.1	.1	.1
3360	99.0	99.6	99.6	99.7	.6	.3	.4	.2	.1	.2	.1
2400*	96.6	98.8	98.9	99.0	1.6	.8	.8	.7	.1	.3	.2
1700	91.8	96.8	97.0	97.2	2.9	1.8	1.8	1.6	.2	.5	.3
1200*	84.0	93.0	93.0	93.2	4.4	3.4	3.3	3.1	.2	.5	.4
850	73.1	86.4	86.0	86.1	5.5	5.2	5.1	5.0	.5	.6	.4
600	59.6	76.3	75.8	75.9	6.1	6.7	6.5	6.7	.6	.8	.4
425	44.5	62.8	62.8	62.9	5.5	7.1	7.0	7.5	.2	1.0	.8
300	31.6	48.7	49.5	49.7	4.2	6.2	6.3	7.1	.8	1.6	1.0
212	23.9	38.8	39.0	39.3	3.5	5.3	5.3	6.2	.3	1.4	.6
150*	18.4	30.7	30.9	31.2	3.1	4.4	4.4	5.4	.2	1.3	.2
106	14.5	24.6	24.6	24.9	2.9	3.7	3.7	4.7	.2	1.2	.2
75	11.9	20.1	19.8	20.0	2.5	3.1	3.1	4.0	.4	1.1	.5
53	10.2	17.2	16.1	16.3	2.3	2.7	2.6	3.3	1.1	1.3	.8

* Interpolated data

**Standard variation = $[\Sigma(M-\overline{M})^2/26]^{0.5}$ or $[\Sigma(P-\overline{P})^2/26]^{0.5}$

***Standard error = $[\Sigma(P-M)^2/26]^{0.5}$

5. POSSIBLE MODEL EXTENSIONS

Simulation outside the normal range is usually not required for mill control. However, for scale-up and design, the following plausible relationships are offered. They were extracted from a literature search and could not be validated with the Brenda Mines data set. Therefore, they should be used with reservation.

Relationships

The selection function is proportional to power draw (7,21):

$$S_i = S_i^e(P/H)$$

P = mill power draw (kW)
H = mill holdup mass (t)
S_i^e = proportionality constant (t/kWh)

The selection function is inversely proportional to the Bond work index (22):

$$S_i = (K_i W_i)(P/H)$$

W_i = Bond work index (kWh/t)
K_i = dimensionless constant

Power draw varies with operating conditions (22):

$$P/H = K_b D^{0.3} \Theta_c (1 - 0.937\, J)\,[1 - 0.1/(2^{9-10\Theta c})]$$

K_b = proportionality constant
D = mill diameter
Θ_c = fraction of mill critical speed ($\approx$0.7)
ΘJ^c = apparent fraction of mill filled by balls ($0.2 < J < 0.6$)

Holdup mass varies with mill geometry (21):

$$H = K_H D^2 L$$

K_H = proportionality constant
L = mill length

6. CONCLUSIONS

Ball mill models have rarely benefitted from examination with a large industrial database. But now, the utility of a kinetic model has been proved using 100 sets of industrial data collected from two different mines and spanning a period of two years at each mine. The selected model is described in the introduction, but can be abbreviated mathematically as:

$$\left\{\begin{array}{l}\text{weight fraction in}\\ \text{size interval "i" of}\\ \text{production mill discharge}\end{array}\right\} = P_i^c = \int_{t=0}^{\infty} h(t)P_i(t)dt$$

where $p_i(t)$ is the solution of the batch-grinding equation:

$$\frac{dP_i(t)}{dt} = -(S_iH)P_i(t) + \sum_{j=1}^{i-1} b_{ij}(S_jH)P_j(t)$$

In these equations the following apply:

- The breakage function b_{ij} is non-normalizable for both the Brenda and Bell Copper ore.
- The residence time distribution h(t) is more than adequately modelled by a three-perfect-mixers-in-series-plus-plug-flow mixing model.

7. REFERENCES

1. Epstein, B. "Logarithmico-normal distribution in breakage of solids"; *Ind Eng Chem* 40:12:2289-2291; 1948.

2. Broadbent, S.R., and Callcott, T.G. "A matrix analysis of processes involving particle assemblies"; *R Soc Lond Phil Trans* 249A:99-123; 1956.

3. Gardner, R.P., and Austin, L.G. "A chemical engineering treatment of batch grinding"; In *Comminution: 1st European Symposium*, Weinheim, Verlag Chemie, pp. 217-248; 1962.

4. Loveday, B.K. "An analysis of comminution kinetics in terms of size distribution parameters"; *J S Afr Inst Min Metall* 68:3; 1967.

5. Gupta, V.K.; Hodouin, D.; and Spring, R. "SPOC Manual: Chapter 7.2: FINDBS computer program for breakage and selection functions determination in the kinetic model of ball mills"; *Report* SP85-1/7.2; CANMET, Energy, Mines and Resources Canada; 1985.

6. Reid, K.J. "A solution to the batch grinding equation"; *Chem Eng Sci* 20:953; 1965.

7. Fuerstenau, D.W. "Research on comminution processes and simulation"; *Report* 51:39-79; USBM; 1978.

8. Austin, L.G.; Klimpel, R.R.; Luckie, P.T.; and Rogers, R.S.C. "Design and installation of comminution circuits"; In *Simulation of Grinding Circuits for Design*; p. 24; edited by A. Mular and G. Jergensen; Soc Min Eng Am Inst Min Metall Pet Eng; 1982.

9. Marchand, J.C.; Hodouin, D.; and Everell, M.D. "Residence time distribution and mass transport characteristics of large industrial grinding mills"; In *Proc 3rd IFAC Symp* on Automation in Mining, Mineral and Metal Processing; Pergamon Press; Montreal, Canada; 1980.

10. Larsen, C. *1975 Brenda Mines Data*; received from C. Larsen; Brenda Mines Ltd.; December 1981.

11. Larsen, C. *1977 Brenda Mines Data*; received from C. Larsen; Brenda Mines Ltd.; December 1981.

12. Wong, K. *1977 Bell Copper Data*; University of British Columbia; 1981.

13. Larsen, C. *1979 Bell Copper Data*; received from C. Larsen; Brenda Mines Ltd.; December 1981.

14. Klimpel, R., and Austin, L.G. "The back calculation of specific rate of breakage and non-normalizable breakage distribution parameters from batch grinding data"; *Int J Miner Process* 4:7-32; 1977.

15. Gupta, V.K.; Hodouin, D.; Bérubé, M.A.; and Everell, M.D. "The estimation of rate and breakage distribution parameters from batch grinding data for a complex pyrite ore using a back-calculation method"; *Powder Technol* 28:97-101; 1981.

16. Flament, F.; Hodouin, D.; and Spring, R. "SPOC Manual, Chapter 7.3: RTD&MIXERS computer programs for residence time determination of process units by tracer experiments"; *Report* SP85-1/7.3; CANMET, Energy, Mines and Resources Canada; 1985.

17. Gardner, R.P., and Sukanjnatee, K. "A combined tracer and back calculation method for determining particulate breakage function in ball milling. Part II — Simulation of an open circuit continuous mill system"; *Powder Technol* 7:169-179; 1973.

18. Apling, A.C.; Montaldo, D.H.; and Young, P.A. "The development of a combined comminution — classification — flotation model"; In *CIM XIV International Mineral Processing Congress Preprints*, III:4-12; Toronto; 1982.

19. Austin, L.G., and Weller, K.R. "Simulation and scale-up of wet ball milling"; In *CIM XIV International Mineral Processing Congress Preprints*, I:8-24; Toronto; 1982.

20. Draper, N.R., and Smith, H. *Applied Regression Analysis*; John Wiley & Sons; New York; 1966.

21. Austin, L.G.; Luckie, P.T.; and Klimpel, R.R. "Process engineering of size reduction: Ball milling"; *Soc Min Eng Am Inst Min Metall Pet Eng*; Littleton, Colorado; 1984.

22. Herbst, J.A.; Rajamani, K.; and Kinneberg, D.J. *ESTIMILL — A Program for Grinding Simulation and Parameter Estimation with Linear Models*; University of Utah; 1977.

APPENDIX A

BELL COPPER MILL MODELLING

Additional data from Noranda Mines Limited (Babine Division — Bell Mine) corroborated the conclusions derived from the Brenda Mines data that the absolute selection function is independent of feed rate, feed size distribution, and pulp per cent solids over the normal operating range. The additional grinding circuit data consisted of 37 sets of sampling campaign data collected in 1977 (Reference A1) and a further 16 sets collected in 1979 (Reference A2). The raw data were balanced using BILMAT (Reference A3).

Ore samples for breakage tests were not obtained in either 1977 or 1979, however, samples of the ore milled in 1982 were available. After confirming that the operating work index of the ore had not changed since 1979 (Reference A4), single-size fraction batch grinding tests were done under conditions identical to those described in Section 2.1. The results appear in Table A1.

A six-parameter non-normalized breakage function was determined from the laboratory data. Table A2 gives the breakage distribution function constants, and Table A3 gives a portion of the breakage matrix. The constants were estimated using only the first and second product size distributions for each feed in Table A1. The third set of product-size distributions was not used, because the grinding kinetics became markedly non-first-order as grinding progressed (see Fig. A1). Figure A2 shows the corresponding selection function for the batch experiment.

Only the cubic-type selection function shown in Figure A3 adequately modelled the production mill selection function. When *hump*-type selection functions were fitted to the data, the standard deviation of the residuals was consistently higher. Therefore, modelling efforts concentrated on using the cubic function. To facilitate interpretation of the results, Tables A4 and A5 list the absolute selection function values (grinding rates) for (28/35 M) particles 0.5 mm in diameter and the slopes of the selection functions at 0.5 mm. H_0 was not known for the Bell Copper mills, and so the functions could not be scaled as was done for the Brenda Mill data. For convenience, however, the listed values of S_i (0.5) have been reduced by a factor of 1000. Evidently the selection functions varied much less than the feed rate, feed size distribution or pulp per cent solids did.

In the same tables the standard errors for a model with a variable selection function (SE_b) and for a model with a fixed selection function based on average constants (SE_m) are listed. While the standard deviations for the simple model are higher, they are still reasonably low averaging less than 1%. Table A6 displays the correlation coefficients by screen and demonstrates that the simple model explains most of the variation in product-size distributions. Finally, Tables A7 and A8 list the standard errors per screen. Generally, the model predicted size distributions with better than 1% accuracy.

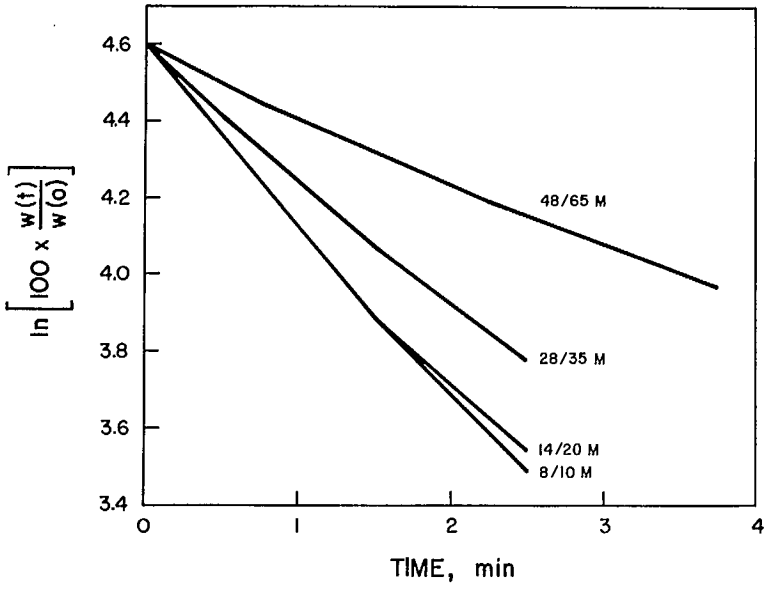

Fig. A1 - First order decay plot — 1982 Bell copper ore

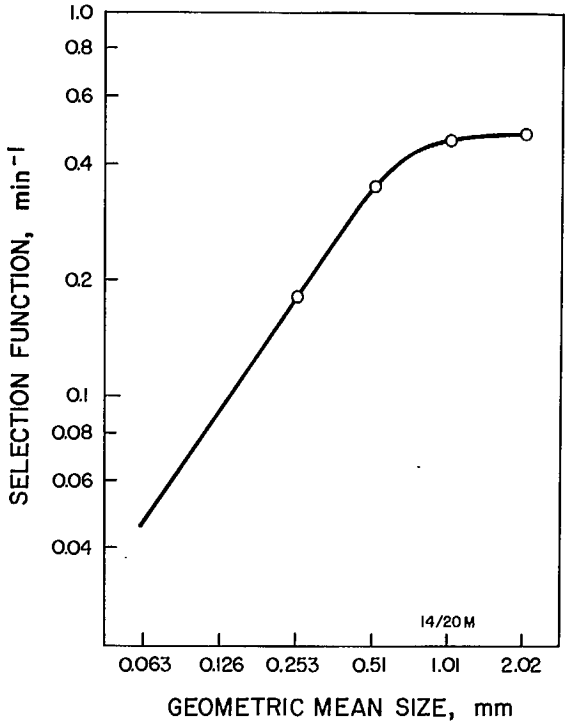

Fig. A2 - Batch mill selection function — 1982 Bell copper ore

Table A1 – 1982 Bell copper single-size fraction breakage test results

		Weight per cent retained on size		
Size (μm)	Feed	0.50-min product	1.50-min product	2.50-min product
1700	75.1	59.8	36.9	24.8
1200	24.1	28.4	33.2	31.3
850	0.1	4.3	10.5	13.5
600	0	1.8	4.9	7.4
425	0	1.0	3.1	5.3
300	0	0.7	2.2	3.6
212	0	0.7	1.8	3.1
150	0	0.5	1.3	1.8
106	0	0.5	1.1	1.7
75	0	0.5	1.2	1.7
53	0	0.4	0.9	1.1
−53	0.7	1.4	2.9	4.7
850	78.2	62.9	38.5	27.2
600	21.1	25.2	30.9	26.1
425	0	4.7	10.6	14.9
300	0	2.1	6.1	9.2
212	0	1.3	3.8	6.1
150	0	0.6	2.2	3.5
106	0	0.6	1.6	2.8
75	0	0.5	1.6	2.6
53	0	0.1	0.8	1.8
−53	0.7	2.0	3.9	5.8
425	73.1	60.6	43.2	32.0
300	24.2	28.2	32.1	31.5
212	2.2	5.6	11.0	14.7
150	0	1.6	3.8	6.1
106	0	1.1	2.7	4.2
75	0	0.9	2.0	3.3
53	0	0.5	1.0	3.1
−53	0.5	1.5	4.2	5.1
212	44.9	38.8	29.9	23.9
150	47.2	46.0	42.6	39.8
106	7.4	10.2	14.0	16.2
75	0.2	2.1	5.3	7.7
53	0	0.7	2.2	3.8
−53	0.3	2.2	6.0	8.6

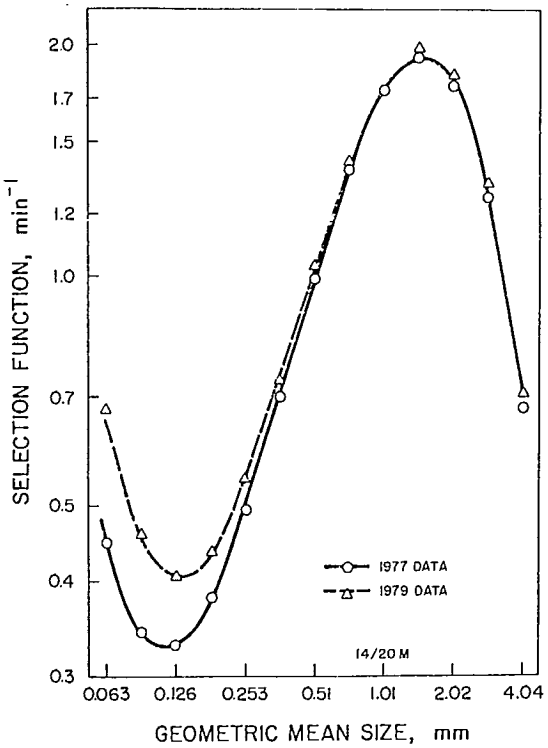

Fig. A3 - Estimated cubic selection functions — 1977 and 1979 Bell copper data

REFERENCES

A1. Wong, K. *1977 Bell Copper Data.* (received from Prof. A. Mular); University of British Columbia; 1981.

A2. Larsen, C. *1979 Bell Copper Data*; Brenda Mines Ltd.; 1981.

A3. Hodouin, D.; Flament, F. "SPOC Manual, Chapter 3.1: Material balance computation for process evaluation and modelling — BILMAT computer program"; *Report* SP85-1/3.1; CANMET, Energy, Mines and Resources Canada; 1985.

A4. Larsen, C. Brenda Mines Ltd; Letter to J. Kazakoff; July 28, 1982.

Table A2 – Breakage function constants — 1982 Bell copper ore

	Value
b_1	.4085
b_2	.8332
b_3	15.49
b_4	.3399
b_5	.0922
b_6	−1.440

Table A3 – Breakage distribution matrix (incomplete) — 1982 Bell copper ore

Size (μm)	2400/1700	1700/1200	1200/850	850/600	600/425	425/300	300/212	212/150	150/106
2400/1700	0								
1700/1200	.742	0							
1200/850	.053	.718	0						
850/600	.041	.065	.692	0					
600/425	.033	.049	.079	.663	0				
425/300	.026	.038	.057	.095	.632	0			
300/212	.021	.029	.043	.066	.113	.597	0		
212/150	.017	.023	.032	.048	.076	.134	.558	0	
150/106	.013	.018	.024	.035	.053	.086	.158	.516	0

Table A4 – Selection function slope and scale — 1977 Bell copper data

Run	$S_i(0.5)$	Slope	Q	%-212 μm	SE_b	SE_m
1	.892	1.045	1029.0	34.0	.3	.8
2	.981	1.044	926.5	39.9	.5	.6
3	.920	1.019	893.5	44.1	.5	1.0
4	.934	.994	985.6	41.0	.3	.5
5	.981	.985	682.3	39.8	.4	.4
6	.972	.971	672.1	42.5	.3	.3
7	.959	1.049	590.7	43.1	.5	1.3
8	.932	1.013	621.9	39.3	.2	.9
9	.981	1.002	652.8	36.6	.3	.4
10	.948	.973	615.7	34.7	.4	.7
11	.975	1.000	550.7	37.3	.3	.7
12	.920	1.051	613.8	39.5	.4	1.3
13	.927	1.020	973.2	37.6	.5	.6
14	.901	.967	753.9	33.9	.4	.9
15	.845	.918	716.6	37.9	.3	1.8
16	.910	1.027	869.9	38.6	.5	1.0
17	.911	1.060	767.4	35.9	.4	.7
18	.853	.983	535.2	30.6	.6	2.2
19	.941	.942	594.5	34.5	.4	.7
20	.916	1.037	833.2	34.4	.4	.7
21	.940	1.037	537.3	38.0	.4	1.5
22	1.004	.967	722.8	42.1	.3	.3
23	1.007	.997	711.5	37.6	.4	.4
24	1.049	1.016	1044.5	39.5	.4	.6
25	.976	1.004	647.0	41.5	.3	.7
26	1.079	1.044	904.1	44.8	.3	.5
27	1.055	1.044	749.5	40.7	.3	.5
28	1.126	1.037	931.8	42.4	.4	.8
29	1.058	.979	959.4	47.8	.3	.5
30	1.031	.979	1025.9	46.2	.2	.4
31	1.065	1.053	977.1	40.3	.3	.8
32	.967	1.078	903.7	37.8	.3	.8
33	1.009	1.093	993.7	41.3	.3	.5
34	1.061	1.104	971.4	37.7	.6	1.0
35	.965	1.170	688.4	45.9	.3	1.2
36	1.080	1.193	852.1	54.0	.4	1.7
37	1.099	1.105	657.3	40.5	.4	.9
Avg	.978	1.027	788.0	39.8	.37	.82
Sd	.069	.057	161.6	4.5	.09	.44

Average cubic selection function parameters

	Value	Std. dev.
s_1	1.740	.1739
s_2	.5281	.1256
s_3	−.5682	.1065
s_4	−.2107	.0279

Table A5 – Selection function slope and scale — 1979 Bell copper data

Run	$S_i(0.5)$	Slope	Q	%S	%-212 μm	SE_b	SE_m
1	.996	1.007	764.8	74.0	29.1	.2	.5
2	.982	.943	869.8	73.3	33.2	.3	.8
3	.985	.998	932.1	74.6	29.4	.4	.5
4	.988	.962	1060.1	75.0	26.4	.7	.7
5	1.074	.967	1162.9	74.7	26.2	.8	1.4
6	1.048	.994	1129.6	72.1	29.9	.7	.7
7	1.045	.996	875.9	76.0	33.0	.5	.6
8	1.042	.950	910.2	75.0	34.7	.5	.9
9	1.129	.989	774.7	76.8	33.0	.5	.9
10	1.049	.999	719.4	69.0	27.5	.7	.5
11	1.071	1.020	645.3	74.1	29.9	.5	.6
12	1.072	.977	696.0	71.8	30.2	.6	.6
13	1.005	1.052	798.3	73.1	33.0	.3	.5
14	.937	.999	874.0	74.2	28.6	.6	1.0
15	.957	.977	1035.4	75.1	24.5	.6	.7
16	.970	.682	1396.6	74.0	26.4	.5	1.0
Avg	1.022	.970	915.3	74.0	29.7	.53	.75
Sd	.052	.081	199.2	1.9	3.0	.16	.24

Average cubic selection function parameters

	Value	Std. dev.
s_1	1.784	.1064
s_2	.5312	.0707
s_3	−.5458	.1128
s_4	−.2208	.0349

Table A6 – Correlation coefficients by screen — Bell copper

	1977 campaigns				1979 campaigns			
	Cumulative		On-size		Cumulative		On-size	
Size (μm)	Best	Modl	Best	Modl	Best	Modl	Best	Modl
4760	—	—	—	—	.786	.659	.537	.385
3360	.799	.798	.799	.798	.772	.688	.688	.646
2400	.879	.819	.868	.768	.917	.886	.951	.935
1700	.889	.829	.870	.815	.969	.959	.980	.973
1200	.964	.899	.786	.735	.998	.989	.936	.953
850	.992	.950	.922	.894	.999	.993	.983	.985
600	.996	.960	.982	.959	.999	.994	.992	.987
425	.998	.966	.989	.963	.999	.993	.991	.968
300	.999	.968	.975	.932	.999	.987	.912	.927
212	.999	.969	.965	.874	.999	.989	.966	.946
150	.999	.968	.984	.971	.998	.993	.957	.951
106	.999	.963	.995	.985	.999	.988	.995	.991
75	.998	.938	.993	.977	.999	.971	.985	.991
53	.990	.827	.980	.970	.996	.967	.924	.915
−53	—	—	.990	.827	—	—	.996	.967

Table A7 – Standard error breakdown by screen — 1977 Bell copper data (Wong)

	Cumulative								On-size		
	Average size distribution				Standard variation				Standard error		
Size (μm)	Feed	Dis.	Best	Modl	Feed	Dis.	Best	Modl	Best	Modl	Modl
3360	99.65	99.94	99.82	99.83	.24	.09	.13	.12	.15	.13	.13
2400*	97.73	99.34	99.22	99.26	.73	.40	.36	.33	.22	.24	.23
1700	95.44	98.65	98.44	98.50	1.57	.75	.68	.63	.40	.45	.22
1200*	90.69	97.01	97.11	97.19	2.39	1.00	1.12	1.03	.32	.49	.45
850	84.28	94.80	94.67	94.79	3.41	1.77	1.74	1.58	.26	.56	.51
600*	77.14	90.85	90.58	90.73	4.13	2.54	2.51	2.29	.35	.74	.26
425	67.16	83.74	83.71	83.91	4.65	3.36	3.33	3.06	.20	.90	.38
300*	53.29	72.00	72.59	72.85	4.94	4.14	4.13	3.85	.63	1.36	.77
212	39.82	58.88	58.98	59.35	4.47	4.25	4.26	4.12	.21	1.16	.45
150*	28.24	45.74	45.61	46.06	3.27	3.53	3.61	3.74	.20	1.00	.38
106	19.52	34.70	34.48	34.98	2.13	2.64	2.69	3.11	.26	.95	.32
75*	13.46	26.26	26.11	26.69	1.32	1.91	1.90	2.51	.19	1.07	.34
53	9.49	20.25	20.35	21.01	1.16	1.61	1.57	2.13	.24	1.43	.50
−53	—	—	—	—	—	—	—	—	—	—	1.43

* Interpolated data.

Table A8 – Standard error breakdown by screen — 1979 Bell copper data

	Cumulative								On-size		
	Average size distribution				Standard variation				Standard error		
Size (μm)	Feed	Dis.	Best	Modl	Feed	Dis.	Best	Modl	Best	Modl	Modl
4760	99.74	99.99	99.79	99.77	.26	.05	.20	.23	.26	.30	.22
3360	98.70	99.89	99.27	99.22	.89	.35	.53	.61	.73	.83	.56
2400	95.13	98.64	98.02	97.96	1.88	.83	.90	1.15	.73	.90	.23
1700*	89.51	96.67	96.14	96.06	2.98	1.69	1.55	1.86	.70	.83	.31
1200	81.67	93.36	93.23	93.19	3.63	2.62	2.43	2.75	.27	.45	.56
850	72.37	88.43	88.72	88.70	4.15	3.68	3.61	3.78	.35	.52	.49
600*	61.91	81.47	81.89	81.87	4.82	5.00	4.93	4.93	.50	.68	.31
425	50.85	72.38	72.46	72.42	4.95	5.91	5.93	5.82	.21	.70	.43
300*	39.95	61.41	61.16	61.14	3.92	5.72	5.87	5.76	.41	.97	.51
212	29.69	49.51	49.17	49.19	3.03	5.19	5.24	5.25	.39	.85	.23
150	20.63	37.65	37.88	37.93	2.39	4.52	4.51	4.79	.34	.68	.74
106	14.47	29.16	29.04	29.13	1.70	3.67	3.65	4.06	.24	.72	.41
75	10.03	22.25	22.50	22.64	1.06	2.79	2.82	3.33	.29	1.00	.54
53	8.37	18.98	18.82	18.96	.94	2.37	2.36	2.92	.27	.88	.47
−53	—	—	—	—	—	—	—	—	—	—	.88

* Interpolated data.

APPENDIX B

AN EXPERIMENT WITH BREAKAGE FUNCTIONS

AN EXPERIMENT WITH BREAKAGE FUNCTIONS

Figure B1 shows that the estimated selection functions deviated strongly from simple power functions. While reduced grinding rates for very large particles have been explained (B1), increased grinding rates for very small particles are not commonly supposed.

It should be remembered that the model selection functions were **not** measured; they were simply chosen, because when used with the laboratory breakage function they most closely predicted the measured product-size distributions. As an experiment, the selection function in Figure B1 was modified by extrapolating it as a simple power function through the fine sizes. Then, the new selection function was used with the Bell copper industrial data to re-estimate breakage functions.

Figure B2 shows a comparison of the breakage function initially estimated from laboratory data to one estimated from industrial data. For all sizes below 14/20 M (1.0 mm) the industrial mill breakage distribution was finer than the laboratory mill distribution. This is a logical result which compensates for the imposed difference in the selection functions.

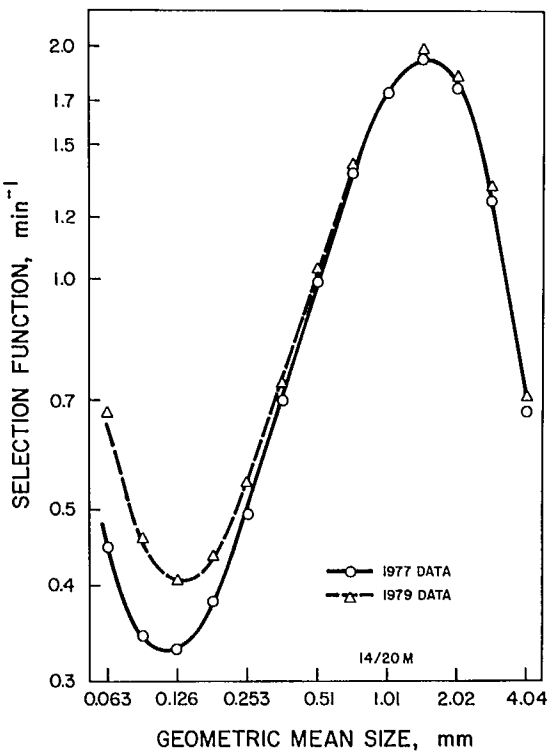

Fig. B1 - Estimated cubic selection functions — 1977 and 1979 Bell copper data

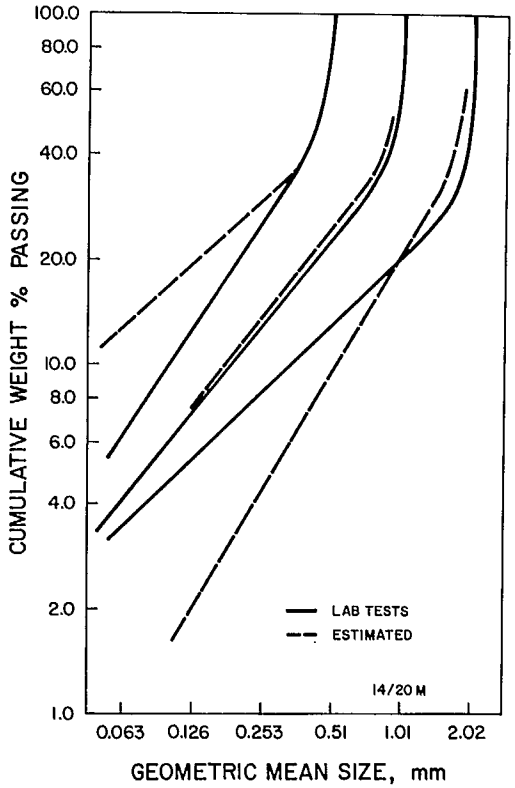

Fig. B2 — Primary breakage distributions — laboratory vs production mill

With the original cubic selection function, the model produced fines by accelerated grinding of 150/200 M and 200/270 M particles. With the modified selection function, the model produced fines by using a finer breakage distribution function. The essential question is: which pair of breakage and selection functions is *correct*; i.e., more representative of the actual grinding mechanism?

REFERENCE

B1. Austin, L.G., Klimpel, R.R., and Luckie, P.T. "The Process Engineering of Size Reduction: Ball Milling." Littleton, Co: *Soc Min Eng Am Inst Min Metall Pet* Eng, 1984.

Canada

Printed in Canada